SCIENCE CHINA
Technological Sciences

• Review •

December 2014 Vol.57 No.12: 2305–2327
doi: 10.1007/s11431-014-5726-7

Progress in optimization of mass transfer processes based on mass entransy dissipation extremum principle

CHEN LinGen[1,2,3*]

[1] *Institute of Thermal Science and Power Engineering, Naval University of Engineering, Wuhan 430033, China;*
[2] *Military Key Laboratory for Naval Ship Power Engineering, Naval University of Engineering, Wuhan 430033, China;*
[3] *College of Power Engineering, Naval University of Engineering, Wuhan 430033, China*

Received October 7, 2014; accepted November 18, 2014

The mass entransy and its dissipation extremum principle have opened up a new direction for the mass transfer optimization. Firstly, the emergence and development process of both the mass entransy and its dissipation extremum principle are reviewed. Secondly, the combination of the mass entransy dissipation extremum principle and the finite-time thermodynamics for optimizing the mass transfer processes of one-way isothermal mass transfer, two-way isothermal equimolar mass transfer, and isothermal throttling and isothermal crystallization are summarized. Thirdly, the combination of the mass entransy dissipation extremum principle and the constructal theory for optimizing the mass transfer processes of disc-to-point and volume-to-point problems are summarized. The scientific features of the mass entransy dissipation extremum principle are emphasized.

mass entransy, finite time thermodynamics, constructal theory, generalized thermodynamic optimization

Citation: Chen L G. Progress in optimization of mass transfer processes based on mass entransy dissipation extremum principle. Sci China Tech Sci, 2014, 57: 2305–2327, doi: 10.1007/s11431-014-5726-7

1 Introduction

With the direct influence of oil crisis in the 1970s, heat transfer enhancement has attracted scientific community's attention all over the world, and became one of the most important subject branches in the field of thermal science and technology quickly. At the same time, the research into identifying the performance limits of thermodynamic processes and optimizing thermodynamic processes has made great progress in the fields of both physics and engineering. In physics, it was termed Finite Time Thermodynamics (FTT) [1–6] by Berry, Andresen and Salamon. While in engineering, according to the Gouy-Stodola theory, the minimum entropy generation of the system denotes the minimum exergy loss, i.e. the thermodynamic performance of the system is the best, and it was termed Thermodynamic Optimization Theory or Entropy Generation Minimization (EGM) [7–10] by Bejan. In addition, Bejan [7–10] believed that the designs of various heat transfer processes could be attributed to the two types of heat transfer enhancement and thermal insulation. The so-called heat transfer enhancement was to improve the system of equivalent thermal conductivity and reduce both the heat transfer temperature difference and the corresponding entropy generation under the condition of the given heat transfer rate; the so-called thermal insulation was to reduce the equivalent thermal conductivity, heat transfer rate and the corresponding entropy generation under the condition of the given heat transfer surface temperature. It was seen that the optimal designs of both heat transfer enhancement and thermal insulation could be attributed to the pursuit of minimum entropy production. Therefore, the "minimum entropy production" was taken as

*Corresponding author (email: lgchenna@yahoo.com, lingenchen@hotmail.com)

an important optimization criterion in the researches of thermodynamic optimization and heat transfer enhancement. It has attracted a large number of scholars' attention, and a lot of valuable research results were gained for practical applications in engineering. In 1996, Bejan [11] further proposed the constructal theory based on the researches of thermodynamic optimization, and applied it into the optimization of high thermal conductivity material distribution in the cooling of electronic components (volume-to-point problem) firstly [12]. Constructal theory, which was also called "non-equilibrium thermodynamic system configuration problem" in the thermal science field, provided a theoretical basis for both the uniform interpretation of the natural tissues to generate the flow structures and the designs of a variety of flow structures.

As a basic heat exchange device, heat exchanger plays an important role in the thermal energy transfer and conversion processes. Thus, it is one of the most important research objects in the fields of thermodynamic optimization and heat transfer enhancement. However, entropy generation denotes the irreversibility of heat-work conversion processes, and the minimum entropy production of the heat exchanger doesn't always correspond to its maximum effectiveness entirely. Bejan [13] analyzed the performance of the balanced counter-flow heat exchanger, and showed that the entropy generation of the heat exchanger increased firstly and then decreased with the increase of its effectiveness. This phenomenon was called the "entropy generation paradox". For the appearance of the "entropy generation paradox", both Xu et al. [14] and Hesselgreaves [15] have proposed different methods for introducing modified and improved entropy generation number. In 1996, Guo et al. [16–18] analyzed the hot and cold fluid temperature fields in different types of heat exchangers, and pointed out that the counter-flow heat exchanger has the most uniform temperature difference field compared with the other heat exchangers, while the parallel-flow heat exchanger has the worst uniform temperature difference field (the maximum and the minimum temperature differences lies at the import and export of the heat exchanger, respectively). As a result, the phenomenological theory "temperature difference field uniformity principle" to optimize the performance of heat exchanger was put forward by Guo et al. [16–18], i.e. the more uniform the temperature difference field is, the larger the effectiveness of the heat exchanger is. In 1998, Guo et al [19–21] further re-examined the physical mechanism of the convective heat transfer, and regarded the energy equation as a heat conduction equation where the convection term was taken as a heat source. They found that the overall strength of the heat sources not only depended on the velocity and the physical features of the fluid, but also depended on the coordination of the flow velocity and heat flow vector. Based on their analysis, they proposed the field synergy principle for convective heat transfer enhancement by changing the coordination relationship between the velocity field and temperature field, which is in favor of searching effective methods for controllable heat exchange.

In 2006, according to the shortcomings of current heat transfer theory and based on the similarity between the heat conduction and electric conduction processes, Guo et al. [22–24] put forward a new physical quantity "entransy" (it was called heat transfer potential capacity [25] in 2003) from the perspective of heat transfer theory. The heat is conserved during the heat transfer process, but the entransy is not conserved and dissipated. The entransy dissipation represents the irreversible extent of heat transfer process. Guo et al. [22–24] also proposed the "entransy dissipation extremum principle", i.e. when the entransy dissipation achieved its extremum for the given constraints, the performance of the heat transfer process is the best. Since the entransy and its dissipation extremum principle have been proposed, it has attracted widespread concerns among domestic and foreign scholars. Some scholars described the physical mechanism of the entransy from different perspectives [26–32], and the entransy theory was applied for the optimization and enhancement of various heat transfer processes such as heat conduction [25,33–54], convection [55–69], radiation [70–75], liquid-solid phase change [76], optimal parameter designs of heat exchangers [77–97], and others [98–103]. Based on the entransy and entransy dissipation function, some new physical quantities including the entransy dissipation number [79,82,87,93,94] and the equivalent thermal resistance [76,80,83] were further defined, which could avoid the entropy generation paradox when they were applied into evaluating the heat exchanger performance and guiding the optimal designs of heat exchangers. This fully reflects the advantages of the entransy theory in the heat transfer performance optimization of heat exchangers. In the performance optimization of heat exchanger associated with heat-work conversion, entropy generation should be chosen as the optimization criterion; while in that only associated with heating and cooling process, entransy dissipation should be chosen as the optimization criterion. This has formed a consensus in the research field [82,89]. The entransy theory could be combined with the finite-time thermodynamics to optimize the heat transfer processes in the heat exchanger and liquid-solid phase change process [76,95–97], and a series of new rules and conclusions were obtained, which were different from those obtained based on entropy generation minimization. The entransy theory could be also combined with the constructal theory to optimize the heat transfer processes and design the structure of heat devices [38–54,67,68,104–113]. Both the equivalent thermal resistance and the average temperature difference of the heat transfer processes and devices could be reduced.

Based on the successful application of the thermal entransy theory into the heat transfer optimization, Chen et al. [114,115] made an analogy between the heat and mass transfer processes, and introduced a new physical quantity, i.e. mass entransy (it was called the mass transfer potential

capacity in refs. [116–118]), into the optimizations of mass transfer processes. Henceforth, many scholars showed great interests in this aspect [119–132].

2 Mass entransy and its dissipation extremum principle

2.1 Thermal entransy and its dissipation extremum principle

To reveal the essence of heat transfer phenomenon, Guo et al. [25] defined heat transport potential capacity and its dissipation function from the viewpoint of heat transfer. They pointed out that the physical meanings of the two definitions were the total amount and dissipation rate of the heat transfer ability, respectively. Through comparing heat conduction with electric conduction as shown in Table 1, Guo et al. [22–24] clarified that the heat transfer potential capacity was a new physical quantity corresponding to the electric potential energy, which described the total heat transfer ability of the object, and called it entransy. The heat transfer ability loss during the heat transfer process was called entransy dissipation. The entransy dissipation extremum principle was also proposed by Guo et al. [22–24]. Since the entransy and its dissipation extremum principle were proposed, a new direction for heat transfer optimization was also opened, and they avoided the limitation and inaccuracy of both the conventional thermal resistance and entropy production to evaluate the heat transfer performance. Guo et al. [24] introduced some new physical quantities such as potential, potential energy, velocity and kinetic energy of heat into heat transfer theory based on analogy with mechanics and electrics, established the conservation equation of thermal motion (considering the motion process of heat as the diffusion process of the phonon gas), and consummated the system of heat transfer theory.

By analogizing heat with electrics as shown in Table 1, Guo et al. [22–24] defined a new physical quantity corresponding to the potential energy in the capacitor, i.e. entransy (ever interpreted as heat transfer potential capacity in ref. [25]):

$$E_h = \frac{1}{2} Q_h T = \frac{1}{2} \rho V c_v T^2, \tag{1}$$

where the subscript "h" denotes the physical quantity related to the heat, the temperature T is an intensive quantity, the thermal capacity $\rho V c_v T$ is an extensive quantity, and the new physical quantity has the meaning of "thermal potential energy". According to that the naming of entropy comes from the ratio of heat to temperature, so the physical quantity was called entransy or thermal entransy. The heat conservation equation for the steady-state heat conduction without the internal heat source is

$$\rho c_v \frac{\partial T}{\partial t} = -\nabla \cdot q, \tag{2}$$

where q is the heat flow density vector. Multiplying both sides of eq. (2) by the temperature T yields

$$\frac{\partial}{\partial t}\left(\frac{1}{2}\rho c_v T^2\right) = -\nabla \cdot (\dot{q} T) + \dot{q} \cdot \nabla T, \tag{3}$$

where ∇T is the temperature gradient. The left side of eq. (3) is the entransy change of the infinitesimal body over the time, and the first term of its right side is the entransy flow into the infinitesimal body, while the absolute value of the second term of its right side is the entransy dissipation rate of the infinitesimal body, i.e. the entransy dissipation function ϕ_h [22–24]:

$$\phi_h = -\dot{q} \cdot \nabla T. \tag{4}$$

The entransy dissipation function denotes the irreversibility of heat transfer ability loss. When the heat transfer

Table 1 Analogies between electrical and thermal parameters [22–24]

Electrical charge stored in a capacitor	Electrical current (charge flux)	Electrical resistance	Capacitance
U_e	I	q_e	R_e
[V]	[C/s]=[A]	[C/(m^2·s)]	[V·s/C]
Heat stored in a body	Heat flow	Thermal resistance	Heat capacity
U_h=T	$\dot{Q}_h$	$\dot{q}_h$	R_h
[K]	[J/s]	[J/(m^2·s)]	[s·K/J]
Electrical potential	Electrical current density	Ohm's law	Electrical potential energy in a capacitor
Q_e	C_e	$q_e = -k_e \frac{dU_e}{dn}$	E_e=($Q_e U_e$)/2
[C]	[F]		[J]
Thermal potential (temperature)	Heat flux density	Fourier law	
U_h=T	$\dot{Q}_h$	$q_h = -k_h \frac{dU_h}{dn}$	?
[K]	[J/s]		

obeys Fourier heat conduction law, eq. (4) becomes

$$\phi_h = \lambda \left|\nabla T\right|^2, \tag{5}$$

where λ is the thermal conductivity. From eq. (4), the entransy dissipation rate over the entire volume is given by

$$\dot{E}_{h\phi} = \int_V \phi_h \mathrm{d}V. \tag{6}$$

Based on the concept of the entransy and its dissipation, the heat transfer efficiency η_{E} (i.e. the entransy transfer efficiency) is given by

$$\eta_E = \frac{E_{h,out}}{E_{h,in}} = \frac{E_{h,in} - E_{h\phi}}{E_{h,in}} = \frac{E_{h,out}}{E_{h,out} + E_{h\phi}}. \tag{7}$$

From eq. (7), when the entransy flow input $E_{h,in}$ or entransy flow output $E_{h,out}$ is specified, the smaller the entransy dissipation $E_{h\phi}$ is, the higher the entransy transfer efficiency η_{E} will be. Cheng et al. [33] used the weighted residual method from the differential equation of heat conduction, and established the variational principle corresponding to the entransy. It pointed out that for the given heat flow condition, the temperature difference of heat conduction achieved its minimum value when the entransy dissipation rate of the object achieved its minimum value. The corresponding expression is

$$\dot{Q}_h \delta(\Delta T) = \delta \int_V \frac{1}{2} k (\nabla T)^2 \,\mathrm{d}V = 0. \tag{8}$$

For the given temperature difference condition, the heat flow of heat conduction achieved its maximum value when the entransy dissipation rate of the object achieved its maximum value. The corresponding expression is

$$\Delta T \delta \dot{Q}_h = \delta \int_V \frac{1}{2} k (\nabla T)^2 \,\mathrm{d}V = 0. \tag{9}$$

Refs. [22–24] summarized them as the entransy dissipation extremum principle, i.e. "For certain constraints and the given boundary condition of heat flow, the performance of heat conduction process is the best (i.e. the temperature difference is the minimum) when the entransy dissipation achieves its minimum value, while for the given boundary condition of temperature, the performance of heat conduction process is best (i.e. the heat flow is the maximum) when the entransy dissipation achieves its maximum value". Based on the entransy dissipation concept, the equivalent thermal resistance R_E for the complex multi-dimensional heat conduction problem is given by

$$R_E = \frac{\dot{E}_h}{\dot{Q}_h^2} = \frac{(\overline{\Delta T})^2}{\dot{E}_h}, \tag{10}$$

where $\dot{Q}_h$ is the heat flow rate pass through the boundary of control volume, $\overline{\Delta T}$ is the average temperature difference. The entransy dissipation extremum principle can be attributed to the minimum thermal resistance principle [22–24], and is described as: "For the heat conduction problem with certain constraints (such as adding a certain amount of high thermal conductivity material into substrate), if the equivalent thermal resistance of the object is the minimum, the heat conduction performance of the object is the best (i.e. the heat flow is the maximum for the given temperature difference condition, or the temperature difference is the minimum for the given heat flow condition".

2.2 Mass entransy and its dissipation extremum principle

For the mass transfer process, the mass fraction c of some component in the mixture is the intensive quantity, while the total mass ρVc of the component is the extensive quantity. According to the analogy between heat and mass transfer processes, Chen et al. [114,115] defined the mass entransy E_m (it was called the mass transfer potential capacity in refs. [116–118]) to describe the diffusion ability of the component in the mixture to its surrounding medium:

$$E = \frac{1}{2} mc = \frac{1}{2} Mc^2 = \frac{1}{2} \rho V c^2, \tag{11}$$

where m is the total mass of the component in the mixture and $m=Mc=\rho Vc$. According to the law of mass conservation and for the transient-state diffusion process without internal mass source, the mass diffusion equation of the component in the mixture is given by

$$\frac{\partial(\rho c)}{\partial t} = -\nabla \cdot (g). \tag{12}$$

When the mass fraction c of the component or effect of the component mass transfer on the mixture density ρ is small, the mixture density of the control volume keeps constant, i.e. ρ=const. Eq. (12) further becomes [114–119]

$$\rho \frac{\partial c}{\partial t} = -\nabla \cdot (g), \tag{13}$$

where g is the mass flow density vector. Multiplying both sides of eq. (13) with the mass fraction c yields

$$\frac{\partial}{\partial t}\left(\frac{1}{2}\rho c^2\right) = -\nabla \cdot (gc) + g \cdot \nabla c, \tag{14}$$

where ∇c is the mass fraction gradient. The left term of eq. (14) is the time variation of the mass entransy stored per unit volume. The first term on the right is the rate of the mass entransy transfer associated with the component diffusions, while the absolute value of the second term on the right is the local rate of mass entransy dissipation. When the mass diffusion process is in steady state, the left term of eq. (14) is equal to zero. In this case, the mass entransy flow calculated from the inlets and outlets of the unit volume in eq. (14) is equal to the mass entransy dissipation calculated

from the mass diffusions between the high and low concentration streams. The mass entransy dissipation rate denotes the irreversible loss due to the concentration gradient during the component diffusion process, and measures the irreversibility of the component diffusion process. The mass entransy dissipation function ϕ_m is given by [114–119]

$$\phi_m = -g \cdot \nabla c. \tag{15}$$

When the mass transfer process obeys Fick's diffusive mass transfer law, eq. (15) becomes [114–119]

$$\phi_m = \rho D \left|\nabla c\right|^2, \tag{16}$$

where D is the diffusive mass transfer coefficient. From eq. (15), the mass entransy dissipation rate $E_{m\phi}$ over the entire volume is given by

$$\dot{E}_{m\phi} = \int_V \phi_m \mathrm{d}V. \tag{17}$$

It should be noted that the above entransy dissipation function was derived based on the mass diffusion equation without internal mass source and the fact that the mass transfer does not affect the density ρ of the control volume [114–119]. When the density ρ changes during the mass transfer process, i.e. $\rho=\rho(c)$, one has to derive the mass entransy dissipation function from the definition of the mass entransy [127,132]. Similarly, based on concepts of the mass entransy and its dissipation, the mass transfer efficiency η_E (the mass entransy transfer efficiency) can be defined, as follows:

$$\eta_E = \frac{E_{m,out}}{E_{m,in}} = \frac{E_{m,in} - E_{m\phi}}{E_{m,in}} = \frac{E_{m,out}}{E_{m,out} + E_{m\phi}}. \tag{18}$$

From eq. (18), it can be seen that for the given mass entransy flow input $E_{m,in}$ or mass entransy flow output $E_{m,out}$, the smaller the entransy dissipation $E_{h\phi}$ is, the larger the mass entransy transfer efficiency η_E is.

Chen et al. [114,115] optimized the convective mass transfer process, and established the mass dissipation extremum principle, namely: "For certain constraints and given mass flow boundary conditions, the performance of mass transfer process is the best (i.e. the concentration difference is the minimum) when the mass entransy dissipation achieves its minimum value, while for the given concentration boundary conditions, the performance of mass transfer process is the best (i.e. the mass flow is the maximum) when the mass entransy dissipation achieves its maximum value". Based on the concept of mass entransy dissipation, the equivalent mass resistance for the complex multi-dimensional mass transfer problem is defined, as follows:

$$R_E = \frac{\dot{E}_m}{\dot{G}^2} = \frac{(\overline{\Delta c})^2}{\dot{E}_m}, \tag{19}$$

where $\dot{G}$ is the mass flow rate pass through the boundary of the control volume, and $\overline{\Delta c}$ is the average concentration difference. Similarly, the mass entransy dissipation extremum principle can be attributed to the principle of minimum mass resistance principle, which is expressed as: "For the mass transfer problem with certain constraint conditions, if the equivalent mass resistance of the control volume achieves its minimum value, its mass transfer performance is the best (the mass flow is the maximum for fixed concentration difference, or the concentration difference is the minimum for given mass flow)".

3 Combination of the mass entransy dissipation extremum principle and the finite-time thermodynamics

Finite time thermodynamics [4,7–10,133–157] is the combination of thermodynamics, heat transfer, fluid mechanics and other transport sciences. The main goal of this theory is to reduce both the irreversibilities of various transfer processes induced by finite potential differences (concentration difference, pressure difference, chemical potential difference, etc.) and the loss of useful work. It is a physical theory to optimize practical processes, cycles and devices with the irreversibilities of heat and mass transfer, fluid flow and other transport phenomena. It is also called "thermodynamic optimization" or "entropy production minimization" in engineering. It can be seen that the mass entransy dissipation extremum principle provides a new theoretical basis for the optimizations of various mass transfer processes induced by the finite potential difference, which is different from that provided by the entropy generation minimization, and opens up a new research direction for finite time thermodynamics. Combination of the mass entransy dissipation extremum principle and the finite-time thermodynamics could be used to optimize the mass transfer processes of one-way isothermal mass transfer, two-way isothermal equimolar mass transfer, isothermal throttling and isothermal crystallization etc., and the obtained results are different from those obtained by entropy generation minimization.

3.1 Mass entransy dissipation minimization for one-way isothermal mass transfer process [127,128]

Figure 1 shows the model of one-way isothermal mass transfer process. Both of the mixtures at the high- and the low-concentration sides are binary. The component that participates in the mass transfer process is called the key component, and the other is called the inert component. The contact surface between the two mixtures only allows the key component to pass. c_1 and c_2 ($c_1>c_2$) are the key component concentrations (expressed as the mass fraction or mole fraction) corresponding to the mixtures at the high- and the low-concentration sides, respectively. m_1 and m_2 are the amount of the flow rates per unit length (expressed as the mass flow

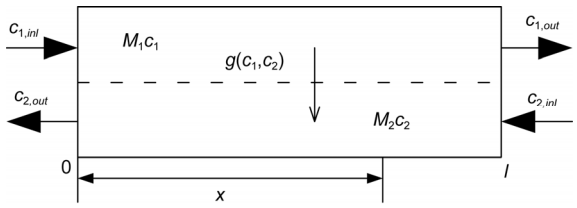

Figure 1 Model of one-way isothermal mass transfer process.

rate or mole flow rate per unit length) of the key components. M_1 and M_2 are the total amount of the flow rates per unit length (expressed as the mass flow rate or mole flow rate per unit length) of the mixtures. l is the total length of the mass transfer equipment. The mass transfer rate between the high- and the low-concentration sides is g, which satisfies the relation $g=-\mathrm{d}m_1/\mathrm{d}x=\mathrm{d}m_2/\mathrm{d}x$.

From eq. (11), the mass entransy E of the key component is given by

$$E=\frac{1}{2}mc=\frac{1}{2}Mc^2, \tag{20}$$

where c is the key component concentration in the mixture. When the concentration c is expressed as the mass fraction, m and M are the mass of the key component in the mixture and the total mass of the mixture, respectively; when the concentration c is expressed as the mole fraction, m and M are the mole numbers of the key component in the mixture and the total mole number of the mixture, respectively. The mole mass of the key component only depends on its physical characteristic, so the expression of the mass fraction is equivalent to that of the mole fraction. The mass entransy E could be used to represent the ability of the key component in a mixture for transferring mass to outside. From eq. (20), one further obtains the change of the mass entransy E, as follows:

$$\mathrm{d}E=\mathrm{d}\left(\frac{1}{2}mc\right)=\frac{1}{2}m\mathrm{d}c+\frac{1}{2}c\mathrm{d}m, \tag{21}$$

where the first term on the right ride of the second equal sign is the change of the mass entransy due to the change of the key component concentration, and the second term on the right ride of the second equal sign is the change of the mass entransy due to the change of the amount of the key component. The mixture consists of two parts, which include the key component and the inert component. Let the amount of the inert component in the mixture be $\tilde{m}$, one further obtains

$$\tilde{m}=M(1-c)=m(1-c)/c. \tag{22}$$

Eq. (22) further gives

$$m=\frac{\tilde{m}c}{(1-c)}. \tag{23}$$

Differentiating eq. (23) with respect to the concentration c yields

$$\mathrm{d}m=\frac{\tilde{m}\mathrm{d}c}{(1-c)^2}. \tag{24}$$

Substituting eqs. (23) and (24) into eq. (21) yields

$$\mathrm{d}E=\left(c-\frac{c^2}{2}\right)\mathrm{d}m. \tag{25}$$

Integrating the left and right sides of eq. (25) along the length of the equipment at both the high- and low-concentration sides, respectively, yields

$$\begin{aligned}\Delta E_1&=E_{1,inl}-E_{1,out}=\frac{1}{2}m_{1,inl}c_{1,inl}-\frac{1}{2}m_{1,out}c_{1,out}\\&=\int_0^l\left[g\left(c_1-\frac{c_1^2}{2}\right)\right]\mathrm{d}x,\end{aligned} \tag{26}$$

$$\begin{aligned}\Delta E_2&=E_{2,out}-E_{2,inl}=\frac{1}{2}m_{2,out}c_{2,out}-\frac{1}{2}m_{2,inl}c_{2,inl}\\&=\int_0^l\left[g\left(c_2-\frac{c_2^2}{2}\right)\right]\mathrm{d}x,\end{aligned} \tag{27}$$

where the three items before the last equal sign in eq. (26) are the differences of the mass entransy flows between the inlet and outlet at the high-concentration side, and the last item in eq. (26) is the mass entransy flow into the low-concentration side. It is the similar situation in eq. (27).

From eq. (14), for the steady state, the mass entransy dissipation can be derived by calculating the mass entransy flows at the inlets and outlets of the equipment. Therefore, the entransy dissipation function ΔE of the mass transfer process can be derived by combining eq. (26) with eq. (27):

$$\begin{aligned}\Delta E&=\Delta E_1-\Delta E_2=E_{inl}-E_{out}=(E_{1,inl}+E_{2,inl})-(E_{1,out}+E_{2,out})\\&=\int_0^l\left[g(c_1-c_2)\left(1-\frac{c_1+c_2}{2}\right)\right]\mathrm{d}x,\end{aligned} \tag{28}$$

where ΔE_1 is the total entransy flow output from the fluid at the high-concentration side, ΔE_2 is the total entransy flow input into the fluid at the low-concentration side, and the difference between them is the entransy dissipation function ΔE of the mass transfer process. Eq. (28) also shows that the total entransy flow E_{out} of the high- and the low-concentration side mixtures at the outlet is smaller than that at the inlet, and the difference between them is the entransy dissipation function ΔE of the one-way isothermal mass transfer process. From eq. (28), the equivalent mass resistance R_E based on the mass entransy dissipation function ΔE during the mass transfer process is obtained, as follows:

$$R_E=\frac{\Delta E}{G^2}=\frac{\int_0^l g(c_1-c_2)\left(1-\frac{c_1+c_2}{2}\right)\mathrm{d}x}{\left[\int_0^l g(c_1,c_2)\mathrm{d}x\right]^2}, \tag{29}$$

where G is the amount of key component mass transfer per unit time for the mass transfer process. R_E measures the effectiveness of the mass transfer process. The smaller R_E is, the better the effectiveness of the mass transfer process is. From eq. (29), one can see that optimizing the mass transfer process with the objective of the minimum ΔE is equivalent to that with the objective of the minimum R_E when the total mass transfer amount G is fixed. From eqs. (26)–(28), one further obtains the mass transfer efficiency based on the mass entransy, which is given by

$$\eta_E = \frac{\Delta E_2}{\Delta E_1} = \frac{\Delta E_1 - \Delta E}{\Delta E_1}. \tag{30}$$

If the total mass transfer amount G is given, i.e. both the initial concentration $c_{1,inl}$ and final concentration $c_{1,out}$ of the fluid at the high concentration side are fixed, the total input entransy flow ΔE_1 is also fixed from eq. (26). For the fixed mass transfer amount G, optimizing the mass transfer process with the objective of the minimum entransy dissipation is equivalent to that with the objective of the maximum mass transfer efficiency η_E. In summary, for the given mass transfer amount G, the smaller the entransy dissipation is, the smaller the mass resistance R_E is, and the higher the mass transfer efficiency η_E is.

For the constraint of the given mass transfer amount, the optimality condition corresponding to the minimum entransy dissipation of the mass transfer process is obtained by optimal control theory. Based on the universal optimization results, the two special cases for the linear and diffusive mass transfer laws, i.e. [$g \propto \Delta(\mu)$] and [$g \propto \Delta(c)$], are obtained, respectively. The obtained results are also compared with the strategies of the minimum entropy generation, constant concentration ratio and constant concentration difference operations. The results show that the optimal mass transfer strategy for the minimum entransy dissipation of the mass transfer process with the diffusive mass transfer law is that the product of the square of the key component concentration difference between the high- and the low-concentration sides and the inert component concentration at the low-concentration side is a constant, and the optimization result for the linear mass transfer law is evidently different from that for the diffusive mass transfer law as shown in Figures 2 and 3; the mass transfer strategy of constant driving force operation is close to the optimal mass transfer strategy; since the entropy generation and the entransy dissipation denote different physical meanings, the optimization objective selection for the performance optimization of the mass transfer process depends on the practical thermodynamic system and the corresponding demand. According to Gouy-Stodola theory [23], the minimum entropy generation denotes the minimum available energy loss. For a mass transfer process associated with energy conversion, such as distillation and separation processes [158–164] as well as isothermal chemical engines [165–169], the minimum entropy generation should be chosen as the optimization criterion. For a mass transfer process without energy conversion, such as decontamination ventilation in space station cabins [116,117,119] and evaporative cooling process [120–122], the minimum mass entransy dissipation (at the boundary condition of fixed mass flow) should be chosen as the optimization criterion.

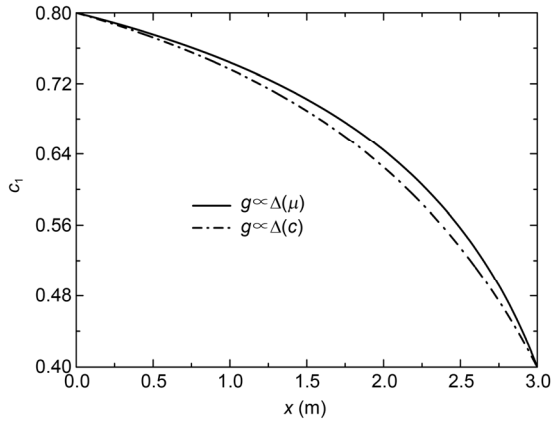

Figure 2 The optimal key component concentration c_1 versus the position x for different mass transfer laws.

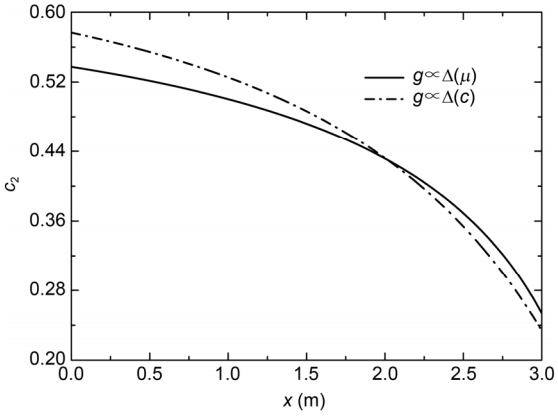

Figure 3 The optimal key component concentration c_2 versus the position x for different mass transfer laws.

3.2 Mass entransy dissipation minimization for two-way isothermal equimolar mass transfer [129]

Figure 4 shows the model of two-way isothermal equimolar mass transfer process. Both of the mixtures at the high- and the low-concentration sides are binary for simplicity (Any inert carrier plays no role, so long as it does not pass from one flow to the other), which are composed of component 1 and component 2, respectively. According to the concentration of component 1, the first fluid is called high-concentration mixture, while the second fluid is called low-concentration mixture. c_1 and c_2 (c_1>c_2) are the key component concentrations (expressed as the mass fraction or mole fraction) corresponding to the mixtures at the high- and the low-

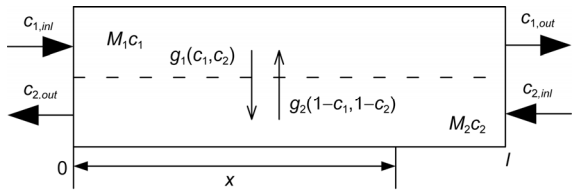

Figure 4 Model of two-way isothermal equimolar mass transfer process.

concentration sides, respectively. m_1 and m_2 are the amount of the flow rates per unit length (expressed as the mass flow rate or mole flow rate per unit length) of component 1. M_1 and M_2 are the total amount of the flow rates per unit length (expressed as the mass flow rate or mole flow rate per unit length) of the mixtures. l is the total length of the mass transfer equipment. The mass transfer flow rate between the high- and the low-concentration sides is g, which satisfies the relation $g= -\mathrm{d}m_1/\mathrm{d}x=\mathrm{d}m_2/\mathrm{d}x$. The mass transfer obeys Fick's diffusive mass transfer law [$g \propto \Delta(c)$], i.e.

$$g_1(c_1,c_2) = -g_2(1-c_1,1-c_2) = g(c_1,c_2) = h(c_1-c_2), \quad (31)$$

where $g_1(c_1,c_2)$ is mass transfer flow rate of component 1, $g_2(1-c_1,1-c_2)$ is mass transfer flow rate of component 2, and h is the mass transfer coefficient. From eq. (31), one further obtains the entransy balance equations corresponding to the high- and low-concentration sides of the mass transfer process, respectively, as follows:

$$\begin{aligned} &E_{1,inl} - E_{1,out} \\ &= \frac{1}{2}M_1c_{1,inl}^2 + \frac{1}{2}M_1(1-c_{1,inl})^2 - \frac{1}{2}M_1c_{1,out}^2 - \frac{1}{2}M_1(1-c_{1,out})^2 \\ &= \int_0^l g(2c_1-1)\mathrm{d}x, \end{aligned} \quad (32)$$

$$\begin{aligned} &E_{2,inl} - E_{2,out} \\ &= \frac{1}{2}M_2c_{2,inl}^2 + \frac{1}{2}M_2(1-c_{2,inl})^2 - \frac{1}{2}M_2c_{2,out}^2 - \frac{1}{2}M_2(1-c_{2,out})^2 \\ &= -\int_0^l g(2c_2-1)\mathrm{d}x. \end{aligned} \quad (33)$$

Combining eq. (32) with eq. (33) yields

$$\begin{aligned} &(E_{1,inl} + E_{2,inl}) - (E_{1,out} + E_{2,out}) \\ &= E_{inl} - E_{out} = \Delta E = 2\int_0^l h(c_1-c_2)^2\mathrm{d}x. \end{aligned} \quad (34)$$

Eq. (34) shows that the total entransy flow E_{out} of the high- and the low-concentration side mixtures at the outlet is smaller than that at the inlet, and the difference between them is called the entransy dissipation function ΔE of the two-way isothermal mass transfer process. The entransy dissipation function ΔE measures the irreversibility of the mass transfer ability loss. For the given mass transfer amount, the smaller ΔE is, the better the effectiveness of the mass transfer process is.

For the constraint of the given mass transfer amount, the optimal concentration allocations of the components corresponding to the high- and the low-concentration sides for the minimum entransy dissipation of the mass transfer process are obtained by applying optimal control theory and compared with the mass transfer strategies of the minimum entropy generation and constant concentration ratio operations. The results show that the optimal mass transfer strategy for the minimum entransy dissipation is that the same component concentration difference between the high- and the low-concentration sides is a constant, which is evidently different from that for the minimum entropy generation [159] as shown in Figure 5. Meanwhile, the mass transfer process studied herein is not involved in energy conversion process significantly, so the optimization principle should be the minimum entransy dissipation. The entransy dissipation of the mass transfer process for the strategy of constant concentration difference is smaller than that for the strategy of constant concentration ratio, so the former is superior to the latter.

3.3 Mass entransy dissipation minimization for isothermal throttling process [130]

Throttling is a particular flow process with notable pressure drop, which is due to local resistance when the gas flows in the pipe. For instance, this process will occur when the gas flows through the tube necking or the adjusting valve. This phenomenon is known as throttling or Joule-Thomson effect. During the adiabatic throttling process, the specific enthalpy decreases with the increase of the flow velocity in the vicinity of shrinkage orifice, and the kinetic energy of fluid increases when the fluid passes through the shrinkage orifice. The pressure drops, and a strong disturbance and friction convert the increase in kinetic energy into heat energy that absorbed by the fluid. Therefore, the specific enthalpy of the fluid before the throttling process is equal to that after the throttling process. The pressure after the throttling process cannot

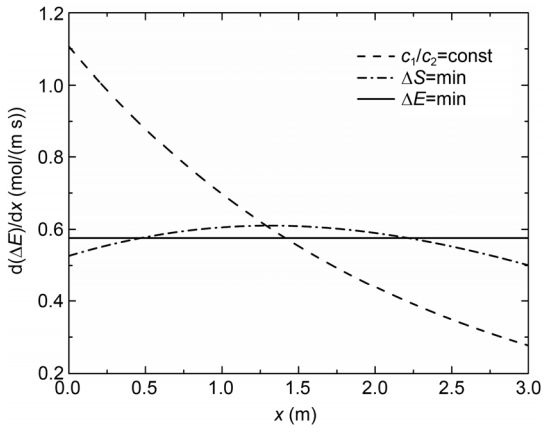

Figure 5 The entransy dissipation density d(ΔE)/dx versus the position x for two-way isothermal equimolar mass transfer process under various mass transfer strategies.

turn back to that before the throttling process due to the irreversibility of the disturbance and friction, so the adiabatic throttling process is irreversible. Strong disturbance and vortex occur near the orifice, the fluid lies in an extreme imbalance state as shown in Figure 6. The state near the orifice cannot be analyzed by using the equilibrium thermodynamics. But in a place far away from the orifice, such as sections 1-1 and 2-2 as shown in Figure 6, the fluid is still in an equilibrium state. It could be analyzed by using the equilibrium thermodynamics. The temperature change of the fluid (liquid, gas) before and after the adiabatic throttling process is called the temperature effect of the throttling, which could be characterized by the adiabatic throttling coefficient or Joule-Thomson coefficient μ_J. Its physical meaning is the temperature change value per unit pressure drop, as follows:

$$\mu_J = \left(\frac{\partial T}{\partial p}\right)_h = \frac{T\left(\frac{\partial V}{\partial T}\right)_p - V}{c_p}. \tag{35}$$

After throttling process, the pressure of the fluid is decreased. From eq. (35), when $\mu_J>0$, the temperature of the fluid is decreased after the throttling process, and this phenomenon is called throttling cold-effect. When $\mu_J<0$, the temperature of the fluid is increased after the throttling process, and this phenomenon is called throttling hot-effect. When $\mu_J=0$, the fluid temperatures before and after the throttling process are equal to each other, and this phenomenon is called throttling zero-effect. For ideal gas, the adiabatic throttling process is the throttling zero-effect due to that $T(\partial V/\partial T)_p = V$.

In ref. [188], the mass entransy dissipation of an isothermal transport network is defined as $\Delta E = F^* \overline{\Delta P}$, where F^* is the injecting flow of the transport network, and $\overline{\Delta P}$ is the weighted average potential difference. Consider a one-dimensional isothermal gas expansion process, the pressure drops from p_1 to p_2, and the rate of expansion depends on the pressure difference. In this process, the gas flow rate is $g(p_1, p_2)$. Based on the definition of the mass entransy dissipation in ref. [188], the mass entransy dissipation ΔE of the isothermal gas expansion process ($\mu_J=0$) is given by

$$\Delta E = \int_0^\tau g(p_1, p_2)(p_1 - p_2)\mathrm{d}t. \tag{36}$$

The impact of heat exchange with the environment is ignored herein. From eq. (36), one further obtains the mass resistance R_E based on the entransy dissipation ΔE, which is given by

$$R_E = \frac{\Delta E}{G^2} = \frac{\int_0^\tau g(p_1, p_2)(p_1 - p_2)\mathrm{d}t}{G^2}, \tag{37}$$

where G is the total mass transfer amount of the throttling process.

For the constraint of the given mass transfer amount, the optimality condition corresponding to the minimum entransy dissipation of the process is obtained by applying optimal control theory. Based on the universal optimization results, the special cases for the mass transfer law [$g \propto (\Delta p)^m$] and the linear mass transfer law [$g \propto \Delta(\mu)$] are further obtained. The obtained results are also compared with those obtained for the mass transfer strategies of the minimum entropy generation, constant pressure ratio and constant pressure difference operations. The results show that the pressure difference between the high- and low-pressure sides with the mass transfer law [$g \propto (\Delta p)^m$] based on minimum mass entransy dissipation is a constant (Δp=const), which is different from that based on minimum entropy generation evidently. The entropy generation for the mass transfer strategy of $\Delta\mu$=const is smaller than that of Δp=const, which reflects that the driving force of the mass transfer process expressed by the entropy is the chemical potential difference. The mass entransy dissipation for the mass transfer strategy of Δp=const is smaller than that of $\Delta\mu$=const, which reflects that the driving force of the mass transfer process expressed by the mass entransy is the pressure difference. The mass transfer strategy of p_1-p_2=const is superior to that of $\mu_1-\mu_2$=const in the reduction of mass entransy dissipation. The optimal pressure ratio between the high- and low-pressure sides with the linear mass transfer law [$g \propto \Delta(\mu)$] based on minimum entropy generation is a constant. The mass transfer strategy of $\mu_1-\mu_2$=const is always superior to that of p_1-p_2=const in the linear mass transfer law [$g \propto \Delta(\mu)$], and this result is independent of the selection of the optimization objective (minimum entropy generation or the minimum mass entransy dissipation). This indicates that the constant driving force operation is close to the optimal strategy of the mass transfer. As shown in Figures 7 and 8, the heat transfer laws have significant effects on the minimum mass entransy dissipation of the throttling process and the corresponding

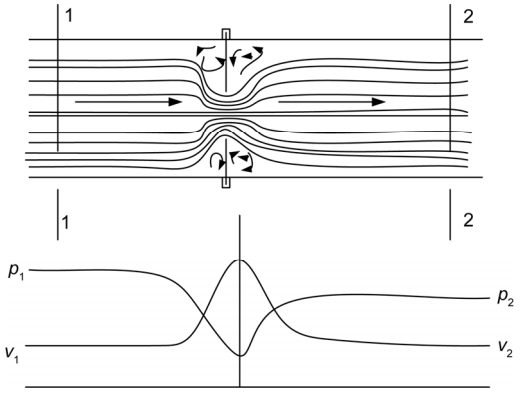

Figure 6 Model of throttling process [170].

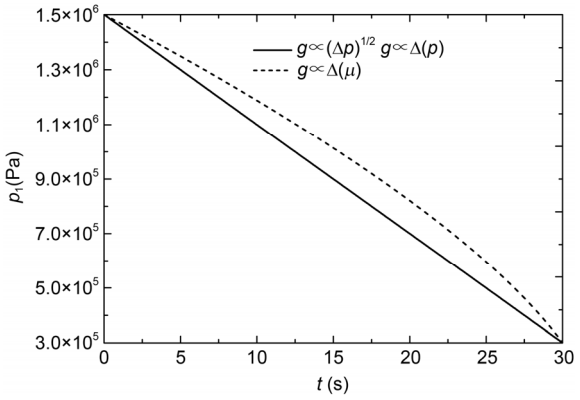

Figure 7 The optimal inlet pressure p_1 versus the time t for different mass transfer laws.

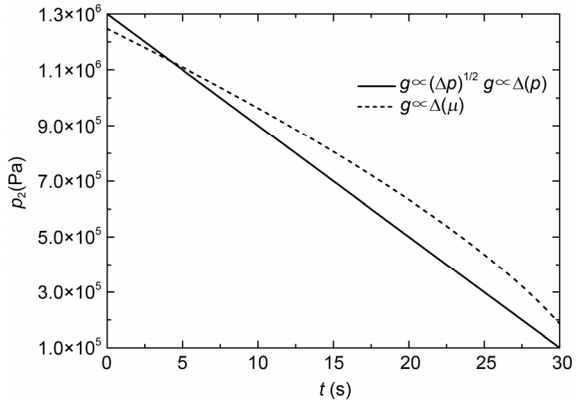

Figure 8 The optimal outlet pressure p_2 versus the time t for different mass transfer laws.

optimal paths of the pressure over the time.

3.4 Mass entransy dissipation minimization for isothermal crystallization [131]

During a crystallization process, the key component crystallizes out of solution on to the surfaces of the crystals already present, where its concentration is higher than the equilibrium concentration in the solution. The initial dimensions (masses) of the crystals are variable, and can be characterized by some distribution. Let the mass transfer rate of the crystallization process be $g(c_1, c_{eq})$. The mass flow rate g depends on the net surface area of the crystals F which, in turn, depends on the mass M of crystals. For a crystal with initial mass $M_i(0)$, the surface $F_i(M_i)$ is proportional to $M_i^{2/3}$ based on the assumption that all of the crystals are sphere. Since the dependence $F_i(M_i)$ is convex as shown in Figure 9, it is guaranteed that the net surface F_Σ, as result of averaging of $F_i(M_i)$ over all M_i, is less than the value of the net surface calculated by assuming that the masses of all the crystals are the same and equal to the average crystal mass at t=0. The mass transfer flow depends monotonically on

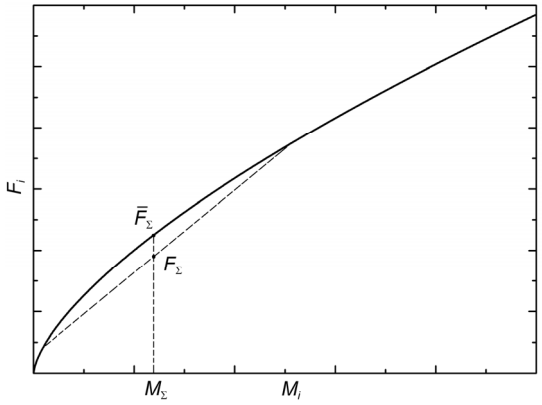

Figure 9 The surface area F_i of the crystal versus its mass M_i.

the mass transfer coefficient, and it increases if the surface of the crystals increases. Therefore the use of the dependence $\bar{F}_\Sigma = KM_\Sigma^{3/2}$ gives low limits on the entropy generation and the entransy dissipation. Assume that both the nucleation and recrystallization don't exist during the crystallization process herein, all of the crystals are the same during the crystallization process. Consider that the crystallization process obeys the mass transfer law $g(M^{2/3}, c_1, c_{eq})$, and then the net mass M of the crystals changes according to the following equation:

$$\frac{\mathrm{d}M}{\mathrm{d}t} = g\left(M^{2/3}, c_1, c_{eq}\right),\ M(0) = M_0,\ M(\tau) = \bar{M}, \tag{38}$$

where τ is the total period of the crystallization process. The entransy dissipation ΔE of the crystallization process is

$$\Delta E = \int_0^\tau g\left(M^{2/3}, c_1, c_{eq}\right)(c_1 - c_{eq})\mathrm{d}t. \tag{39}$$

From eqs. (38) and (39), one further obtains the mass resistance R_E based on the entransy dissipation, which is given by

$$R_E = \frac{\Delta E}{\left(\bar{M} - M_0\right)^2} = \frac{\int_0^\tau g\left(M^{2/3}, c_1, c_{eq}\right)(c_1 - c_{eq})\mathrm{d}t}{\left(\bar{M} - M_0\right)^2}. \tag{40}$$

For the constraint of the given crystals mass, the optimal concentration configuration for the minimum entransy dissipation of the crystallization process is obtained by applying optimal control theory, and the obtained results are also compared with those obtained for the mass transfer strategies of the minimum entropy generation, constant concentration and constant mass flux rate operations. The results show that the 2/3 times net mass of the crystals for the minimum entransy dissipation of the crystallization process with the diffusive mass transfer law changes with time linearly, and the entransy dissipation rate of the process keeps constant, which coincides with equipartition of entransy dissipation [85]; both the minimum entransy dissipation of

the crystallization process with the linear mass transfer law and the corresponding optimal concentration configuration are different from those for the diffusive mass transfer law as shown in Figures 10 and 11; since the crystallization process is not involved in energy conversion process, the optimization principle should be the minimum entransy dissipation.

4 Combination of mass entransy dissipation extremum principle and constructal theory of mass transfer

Since the constructal theory was put forward by Bejan, it has been developed vigorously. Many scholars have shown great interests in constructal theory. Plentiful of researches have been carried out based on this theory, and its content has been greatly enriched. The fields covered by the constructal theory are large, including heat and mass transfer, fluid flow, electricity, magnetism, transport, piping network, efflorescence and torrefaction, economy decision-making, climate forecast, physical geography, economic transportation, product platform design, organization structures and physiology of animals and plants, social dynamics, medical treatment, global security and sustainability, pedestrian dynamics, collection of organism, circulation market dynamics, coastal beach morphology, and so on [171–185]. By combining thermal entransy theory and constructal theory, different results [38–54,67,68,104–109] have been obtained for various kinds of processes with the thermal entransy dissipation rate extremum (minimum or maximum).

Combination of mass entransy dissipation extremum principle and constructal theory for mass transfer process involves constructal optimizations of "disc-to-point" and "volume-to-point" mass transfer. Traditional constructal theory concentrates on the optimization objective of maximum pressure difference minimization which indicates local optimization of porous media [186]. The results based on the minimization of entransy dissipation rate indicate the global optimization of mass transfer in porous media.

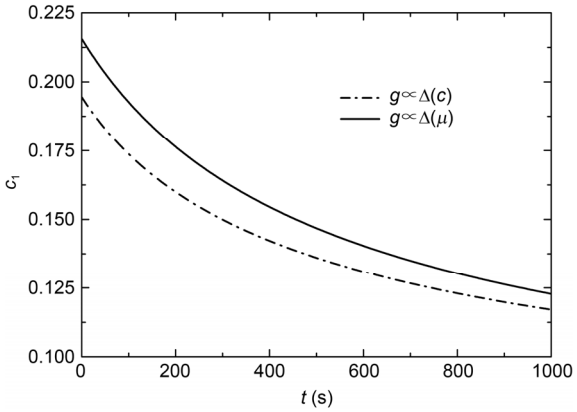

Figure 10 The optimal concentration versus the time for different mass transfer laws.

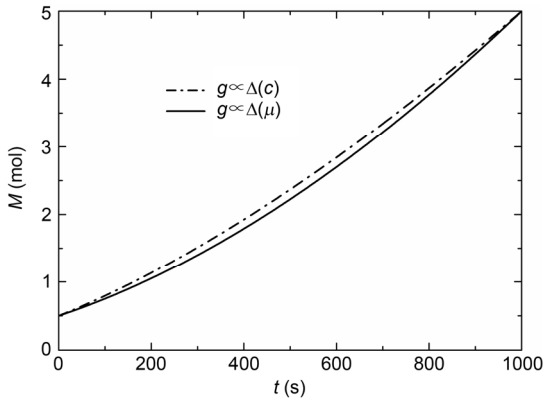

Figure 11 The optimal crystal mass versus the time for different mass transfer laws.

4.1 Mass entransy dissipation rate minimization for "disc-to-point" mass transfer process [187]

4.1.1 Radial-patterned disc

The mass transfer model of radial-patterned disc is as shown in Figure 12. The radius of the disc is R_0 and the permeability is K. The mass current ($\dot{m}' = \dot{m}'''\pi R_0^2$, where $\dot{m}'''$ is the mass generation rate) which is generated uniformly in the disc flows through the high-permeability paths towards the center of the disc. The permeability of the material is K_0 and the thickness is D_0. The number of the high-permeability paths which are distributed uniformly over the disc is N. The pressure of the disc is above P_0.

According to the distribution of high-permeability paths, the disc can be divided into a number of equal sectors, $N=2\pi R_0/(2H_0)$. The radial boundary (dotted line) of each sector is not penetrable. Each sector as depicted in Figure 13 is a fundamental element and N sectors fit in a complete disc arrangement. One assumes $N>>1$ so that each sector is

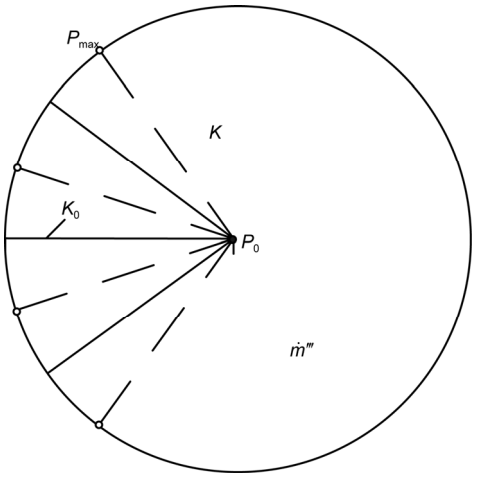

Figure 12 Mass transfer model of radial-patterned disc.

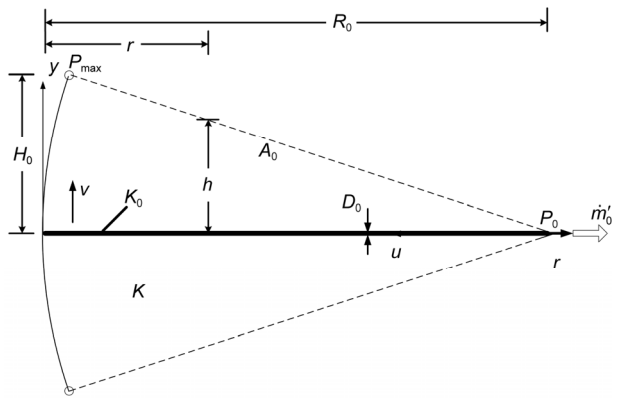

Figure 13 Elemental sector.

sufficiently slender to be approximated by an isosceles triangle of base $2H_0$ and height R_0.

The distribution of pressure difference of the element for $y>0$ is

$$P(r,y)-P_0 = \frac{\dot{m}'''\nu}{K}\left[\frac{H_0}{R_0}(R_0-r)\,y-\frac{y^2}{2}\right]+\frac{2\dot{m}'''\nu}{K_0D_0}\frac{H_0}{R_0}\left(\frac{R_0^3}{3}+\frac{r^3}{6}-\frac{R_0}{2}r^2\right). \tag{41}$$

The entransy dissipation rate of the element is

$$\dot{J}_0 = 2\int_0^{R_0}\int_0^{\frac{H_0}{R_0}(R_0-r)}\dot{m}'''\left[P(r,y)-P_0\right]\mathrm{d}r\mathrm{d}y = \frac{\dot{m}'''^2A_0^2\nu}{K}\left(\frac{1}{6}\frac{H_0}{R_0}+\frac{8}{15\tilde{K}_0\phi_0}\frac{R_0}{H_0}\right), \tag{42}$$

where $\dot{J}$ is entransy dissipation rate of the mass. The mean pressure difference is

$$\Delta\overline{P}_0 = \frac{\dot{J}_0}{\dot{m}_0'} = \frac{\dot{m}_0'\nu}{K}\left(\frac{1}{6}\frac{H_0}{R_0}+\frac{8}{15\tilde{K}_0\phi_0}\frac{R_0}{H_0}\right), \tag{43}$$

and the optimal construct and the corresponding mean pressure difference are, respectively, given by

$$\left(\frac{H_0}{R_0}\right)_{\mathrm{opt}} = \frac{4}{(5\tilde{K}_0\phi_0)^{1/2}} \ll 1, \tag{44}$$

$$\Delta\overline{P}_{0,\min} = \frac{4\dot{m}_0'\nu}{3\sqrt{5}K}(\tilde{K}_0\phi_0)^{-1/2}. \tag{45}$$

The minimal dimensionless mean pressure difference is

$$\Delta\tilde{\overline{P}}_{0,\min} = \frac{\Delta\overline{P}_{0,\min}}{\dot{m}_0'\nu/K} = \frac{4(\tilde{K}_0\phi_0)^{-1/2}}{3\sqrt{5}} = 0.596(\tilde{K}_0\phi_0)^{-1/2}. \tag{46}$$

However, the optimal construct with the minimization of maximum pressure difference and the corresponding dimensionless mean pressure difference are, respectively, given by

$$\left(\frac{H_0}{R_0}\right)_{opt} = \frac{2}{(3\tilde{K}_0\phi_0)^{1/2}} << 1, \tag{47}$$

$$\Delta\tilde{\overline{P}}_{0,p} = \frac{17}{15\sqrt{3}}\left(\tilde{K}_0\phi_0\right)^{-1/2} = 0.654\left(\tilde{K}_0\phi_0\right)^{-1/2}. \tag{48}$$

According to eqs. (44) and (47) it is obtained that the optimal construct of the element based on the minimization of entransy dissipation rate is different from that based on the minimization of maximum pressure difference. From eqs. (46) and (48), one can see that the optimal construct based on the former can decrease the mean temperature difference to a great extent compared with the optimal construct based on the latter, with a clear improvement in the mass transfer performance.

The aspect ratio (i.e. eq. (44)) determines the number of elements which fit in a complete disc arrangement:

$$N_{\mathrm{opt}} = \frac{\pi}{4}(5\tilde{K}_0\phi_0)^{1/2} \gg 1. \tag{49}$$

So eq. (44) shows that the optimal aspect ratio agrees with the above assumption. The radius of the disc is

$$R_0 = \frac{A_0^{1/2}}{2}(5\tilde{K}_0\phi_0)^{1/4}, \tag{50}$$

and the corresponding dimensionless mean mass flow resistance

$$\tilde{\overline{f}}_0 = \frac{\Delta\overline{P}_0}{\dot{m}'''A\nu/K} = \frac{\Delta\tilde{\overline{P}}_0}{N_{\mathrm{opt}}} = \frac{16}{15\pi\tilde{K}_0\phi_0}. \tag{51}$$

The radius of the disc is not determined but results from the optimization, and depends on A_0, ϕ_0 and $\tilde{K}_0$. The product $\tilde{K}_0\phi_0$ is an important quantity. Large $\tilde{K}_0\phi_0$ signifies more high-permeability material, a more slender element and a disc with larger radius.

The number of disc elements in the disc and the radius of the disc based on the minimization of maximum pressure difference are, respectively

$$N_{\mathrm{opt}}' = \frac{\pi}{2}(3\tilde{K}_0\phi_0)^{1/2} \gg 1, \tag{52}$$

$$R_0' = \left(A_0/2\right)^{1/2}(3\tilde{K}_0\phi_0)^{1/4}, \tag{53}$$

and the corresponding dimensionless mean mass flow resistance

$$\tilde{\overline{f}}_{0,p} = \frac{\Delta\tilde{\overline{P}}_{0,p}}{N_{\mathrm{opt}}'} = \frac{34}{45\pi\tilde{K}_0\phi_0}. \tag{54}$$

Comparing eq. (49) with eq. (52), and eq. (50) with eq. (53) one can see that both the number of elements and the

radius of the disc based on the minimization of entransy dissipation rate are smaller than those based on the minimization of maximum pressure difference. That is, the area of the disc based on the minimization of entransy dissipation rate is not equal to that based on the minimization of maximum pressure difference. Therefore, eqs. (51) and (54) are not compared in this paper.

4.1.2 Branch-patterned disc

As shown in Figure 14, the perimeter of the branch-patterned disc is assembled by many elemental sectors of the radial-patterned disc. One K_1 blade (thickness is D_1) stretches radially to a distance R_1 away from the disc center, continues with a number (n) of tributaries (with thickness D_0 and high-permeability K_0) that terminate on the rim.

The distribution of temperature difference of central A_1 sector for $y>0$ is

$$\begin{aligned} &P(r,y)-P_0 \\ &=\frac{\dot{m}'''\nu}{K}\left[\frac{H_1}{R_1}(R_1-r)y-\frac{y^2}{2}\right]+\frac{\dot{m}'''\nu R_1}{K_1D_1}\left(nA_0+\frac{2}{3}A_1\right) \\ &\quad+\frac{\dot{m}'''\nu}{K_1D_1}\left[\frac{2H_1}{R_1}\left(\frac{1}{6}r^3-\frac{R_1}{2}r^2\right)-nrA_0\right]. \end{aligned} \tag{55}$$

The entransy dissipation rate of central sector A_1 is

$$\begin{aligned} \dot{J}_c &= 2\int_0^{R_1}\int_0^{\frac{H_1}{R_1}(R_1-r)}\dot{m}'''\left[P(r,y)-P_0\right]\mathrm{d}r\mathrm{d}y \\ &=\frac{\dot{m}'''^2\nu A_1}{30K\tilde{K}_1D_1}\left(\frac{5\tilde{K}_1D_1}{R_1^{\,2}}A_1^{\,2}+16R_1A_1+20nR_1A_0\right). \end{aligned} \tag{56}$$

The entransy dissipation rate of A_0 element is composed of the entransy dissipation rate introduced by the mass current flowing through A_0 element and the entransy dissipation rate introduced by the mass current flowing through high-permeability blade of central sector A_1, i.e.

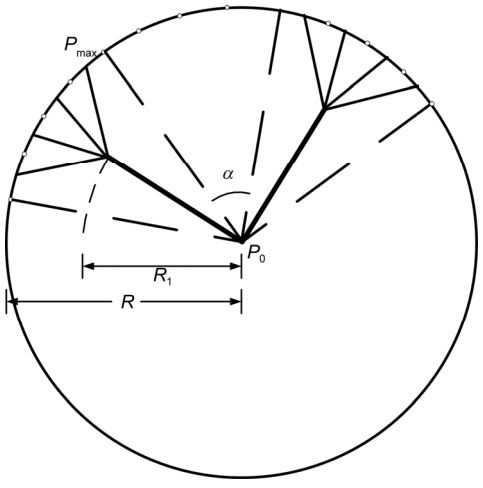

Figure 14 First-order assembly of disc.

$$\dot{J}_p=\frac{4\dot{m}'''^2\nu A_0^{\,2}}{3K}\left(5\tilde{K}_0\phi_0\right)^{-1/2}+\frac{\dot{m}'''^2\nu R_1}{K\tilde{K}_1D_1}\left(\frac{2}{3}A_1+nA_0\right)A_0. \tag{57}$$

The entransy dissipation rate of A sector is

$$\dot{J}_1=\dot{J}_c+n\dot{J}_p. \tag{58}$$

After some mathematical calculations, eq. (58) becomes

$$\begin{aligned} \dot{J}_1=&\frac{n\dot{m}'''^2A_0^{\,2}\nu}{60\tilde{R}^3\tilde{D}K\tilde{K}_1\phi_0}\Big[10n\tilde{R}^2\left(5\tilde{K}_0\phi_0\right)^{3/4}-35n\tilde{R}^3\left(5\tilde{K}_0\phi_0\right)^{1/2} \\ &-80\tilde{R}^3\tilde{D}\left(2n^2-1\right)\tilde{K}_1\phi_0(5\tilde{K}_0\phi_0)^{-1/2}-10n\tilde{R}\tilde{K}_0\phi_0-80n\tilde{R}^6 \\ &+8n\tilde{R}^2(8\tilde{R}^4+15n\tilde{D}\tilde{K}_1\phi_0)(5\tilde{K}_0\phi_0)^{-1/4}-40n^2\tilde{K}_1\phi_0\tilde{R}\tilde{D} \\ &+80n^2\tilde{R}^4\tilde{D}\tilde{K}_1\phi_0(5\tilde{K}_0\phi_0)^{-3/4}+5n(14\tilde{R}^4+n\tilde{D}\tilde{K}_1\phi_0) \\ &\cdot(5\tilde{K}_0\phi_0)^{1/4}\Big], \end{aligned} \tag{59}$$

where $\tilde{D}=D_1/D_0$ is the ratio of thicknesses of high-conductivity blades, and $\tilde{R}=R/A_0^{1/2}$ is the dimensionless radius of the disc. The mean pressure difference of mass transfer is $\Delta\overline{P}_1=\dot{J}_1/(\dot{m}'''A)$, and the corresponding dimensionless mean pressure difference of mass transfer is

$$\begin{aligned} \Delta\tilde{\overline{P}}_1&=\Delta\overline{P}_1/(\dot{m}'''A_0\nu/K) \\ &=\frac{1}{120\tilde{R}^4\tilde{D}\tilde{K}_1\phi_0}\Big[50n\tilde{R}^2\tilde{K}_0\phi_0-35n\tilde{R}^3(5\tilde{K}_0\phi_0)^{3/4} \\ &\quad-80\tilde{R}^3\tilde{D}\left(2n^2-1\right)\tilde{K}_1\phi_0(5\tilde{K}_0\phi_0)^{-1/4}-2n\tilde{R}(5\tilde{K}_0\phi_0)^{5/4} \\ &\quad+8n\tilde{R}^2(8\tilde{R}^4+15n\tilde{D}\tilde{K}_1\phi_0)-40n\tilde{R}(n\tilde{D}\tilde{K}_1\phi_0+2\tilde{R}^5) \\ &\quad\cdot(5\tilde{K}_0\phi_0)^{1/4}+80n^2\tilde{R}^4\tilde{D}\tilde{K}_1\phi_0(5\tilde{K}_0\phi_0)^{-1/2} \\ &\quad+5n(14\tilde{R}^4+n\tilde{D}\tilde{K}_1\phi_0)(5\tilde{K}_0\phi_0)^{1/4}\Big]. \end{aligned} \tag{60}$$

The fraction of the amount of high-permeability K_0 and K_1 materials allocated to the disc is

$$\begin{aligned} \phi_1&=\frac{ND_0R_0+\frac{N}{n}D_1R_1}{\pi R^2} \\ &=\frac{(5\tilde{K}_0\phi_0)^{1/4}\phi_0}{2\tilde{R}}+\frac{\tilde{D}\phi_0}{n\tilde{R}}\left[\tilde{R}-\frac{(5\tilde{K}_0\phi_0)^{1/4}}{2}\right]. \end{aligned} \tag{61}$$

Eq. (61) determines the relationship among n, $\tilde{D}$, $\tilde{R}$, $\tilde{K}_0$ and ϕ_0. Because ϕ_1, $\tilde{K}_0$ and $\tilde{K}_1$ are fixed (e.g., ϕ_1= 0.1, $\tilde{K}_0=1000$ and $\tilde{K}_1=1000$), the relation between $\tilde{D}$ and ϕ_0 is obtained when n and $\tilde{R}$ are given. From eq. (60), one can obtain minimal dimensionless mean pressure difference, $\Delta\tilde{\overline{P}}_{1,\min}$ and the corresponding $\phi_{0,\mathrm{opt}}$ and $\tilde{D}_{\mathrm{opt}}$.

Figure 16 shows the characteristics of the dimensionless mean pressure difference $\Delta\tilde{\overline{P}}_1$ and blade thickness ratio $\tilde{D}$ versus the elemental volume fraction ϕ_0 with n=2,

$\tilde{R}=4$, ϕ_1=0.1 and $\tilde{K}_0=\tilde{K}_1=1000$. The solid and dotted lines represent the analyses based on mean pressure difference and maximum pressure difference ($\Delta\tilde{P}_1$), respectively. From Figure 16, one can see there exist optimal blade thickness ratio ($\phi_{0,\text{opt}}$) and elemental volume fraction ($\tilde{D}_{\text{opt}}$) which lead to minimum $\Delta\tilde{\tilde{P}}_1$ and $\Delta\tilde{P}_1$, respectively. $\phi_{0,\text{opt}}$ obtained based on minimum $\Delta\tilde{\tilde{P}}_1$ is smaller than that based on minimum $\Delta\tilde{P}_1$, but the conclusion is reversed for $\tilde{D}_{opt}$. Therefore, the optimal constructs obtained based on the two optimization objectives are evidently different, and the mean pressure difference is reduced by adopting the former optimal construct. Moreover, the effects of $\tilde{K}_0$, $\tilde{K}_1$, n and $\tilde{R}$ on the optimal constructs ($\phi_{0,\text{opt}}$ and $\tilde{D}_{\text{opt}}$) and optimal flow performances ($\Delta\tilde{\tilde{P}}_{1,\min}$ and $\Delta\tilde{P}_{1,\min}$) are showed in Figures 17–20, respectively.

In each of the cases optimized in Figures 17–20, both the elemental area and dimensionless radius of the disc were fixed. This means that the minimization of dimensionless mean flow resistance of the entire disc is equivalent to the minimization of dimensionless mean pressure difference:

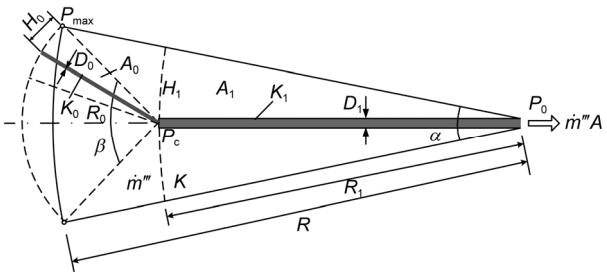

Figure 15 First-order assembly of sector.

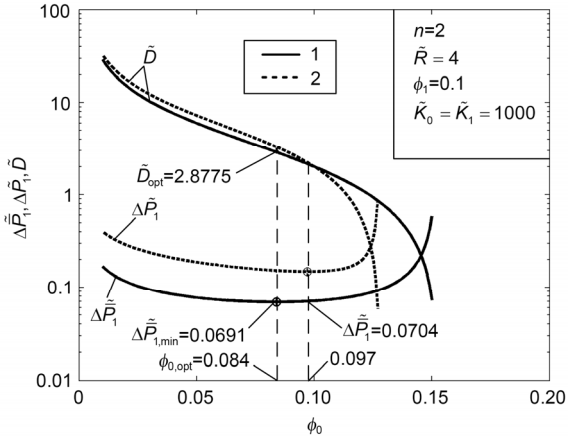

Figure 16 $\Delta\tilde{\tilde{P}}_1$, $\Delta\tilde{P}_1$ and $\tilde{D}$ versus ϕ_0 characteristics. 1, entransy dissipation rate minimization; 2, maximum pressure difference minimization.

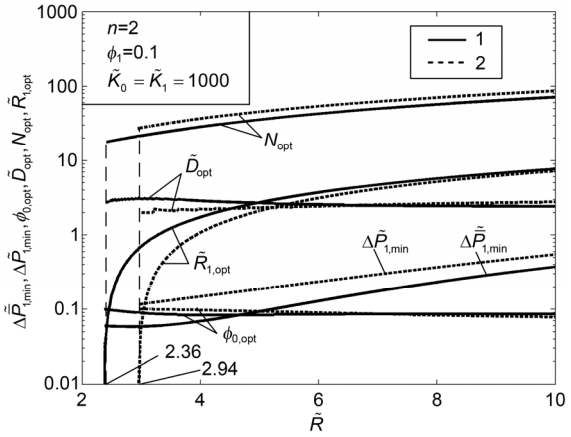

Figure 17 Effect of dimensionless radius $\tilde{R}$ on the optimal construct.

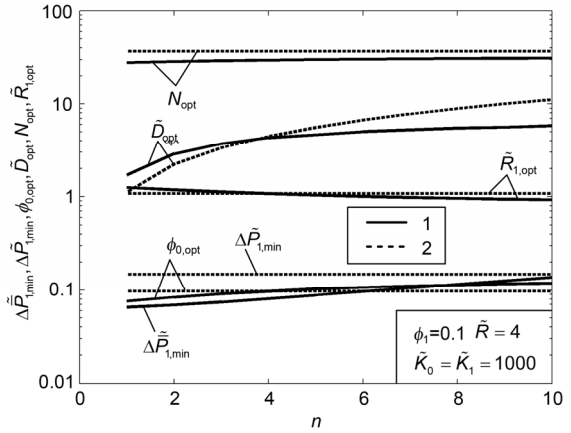

Figure 18 Effect of the number of elemental branches on the optimal construct.

$$\tilde{\tilde{f}}_1=\frac{\Delta\bar{\bar{P}}_1}{\dot{m}'''\pi R^2\nu/K}=\frac{\Delta\tilde{\tilde{P}}_1}{\pi\tilde{R}^2}$$
$$=\frac{1}{120\pi\tilde{R}^6\tilde{D}\tilde{K}_1\phi_0}\Big[50n\tilde{R}^2\tilde{K}_0\phi_0-35n\tilde{R}^3(5\tilde{K}_0\phi_0)^{3/4}$$
$$-80\tilde{R}^3\tilde{D}\left(2n^2-1\right)\tilde{K}_1\phi_0(5\tilde{K}_0\phi_0)^{-1/4}-2n\tilde{R}(5\tilde{K}_0\phi_0)^{5/4}$$
$$+8n\tilde{R}^2(8\tilde{R}^4+15n\tilde{D}\tilde{K}_1\phi_0)-40n\tilde{R}(n\tilde{D}\tilde{K}_1\phi_0+2\tilde{R}^5)$$
$$\cdot(5\tilde{K}_0\phi_0)^{1/4}+80n^2\tilde{R}^4\tilde{D}\tilde{K}_1\phi_0(5\tilde{K}_0\phi_0)^{-1/2}$$
$$+5n(14\tilde{R}^4+n\tilde{D}\tilde{K}_1\phi_0)(5\tilde{K}_0\phi_0)^{1/2}\Big]. \quad (62)$$

Based on the same elemental area and the same amounts and properties of high-permeability materials, one compares $\tilde{\tilde{f}}_{1,\min}$ with $\tilde{\tilde{f}}_0$ as shown in Figure 21. The dimensionless radius of the radial-patterned disc is (cf. eq. (50))

$$\tilde{R}=\frac{(5\tilde{K}_0\phi_1)^{1/4}}{2}. \quad (63)$$

When $\tilde{K}_0$, $\tilde{K}_1$ and ϕ_1 are fixed, the dimensionless radius $\tilde{R}$ can be obtained from eq. (63). The dimensionless

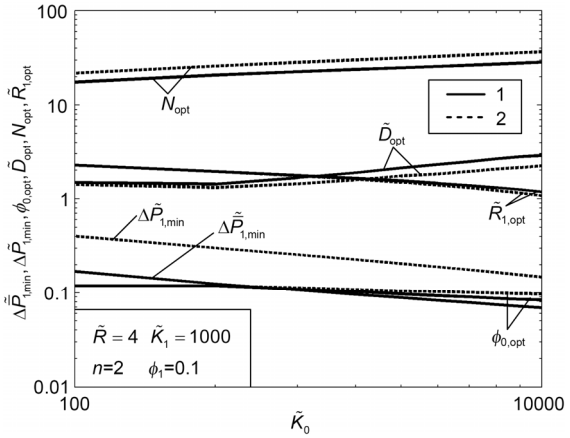

Figure 19 Effect of high-permeability K_0 on the optimal construct.

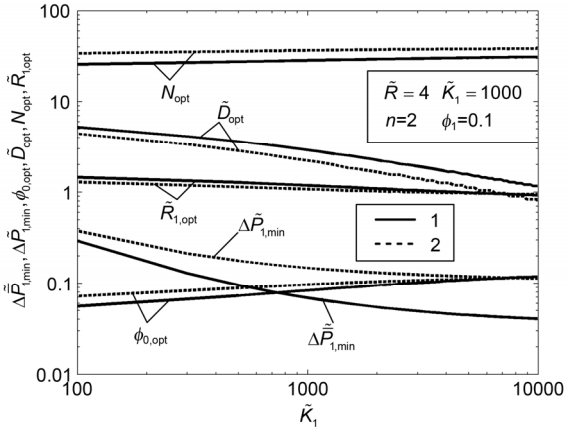

Figure 20 Effect of high-permeability K_1 on the optimal construct.

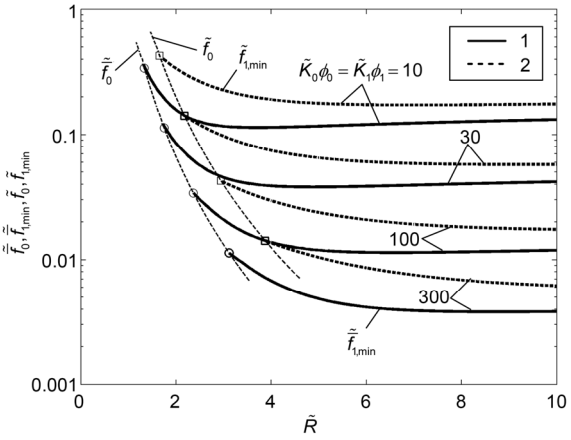

Figure 21 Effects of $\tilde{K}_0$, $\tilde{K}_1$ and ϕ_1 on dimensionless mean flow resistances of radial-patterned and branch-patterned discs.

radius $\tilde{R}$ of a branch-patterned disc in Figure 14 can be free to vary. This is the reason that $\tilde{\tilde{f}}_0(\tilde{R})$ is and $\tilde{\tilde{f}}_{1,\min}(\tilde{R})$ are a point and a curve in Figure 21, respectively. In this figure the dotted line indicates $\tilde{\tilde{f}}_0$ with different $\tilde{K}_0\phi_1$, and the solid lines indicate $\tilde{\tilde{f}}_{1,\min}$ with different dimensionless radius of the branch-patterned disc. From the figure, one can see that when the dimensionless radius $\tilde{R}$ exceeds that of the optimized branch-patterned disc, lower mean flow resistance is achieved when the high-permeability material is distributed according to the branch pattern. The mean flow resistance can also be decreased and the mass transfer performance of the porous media is improved by increasing $\tilde{K}_0\phi_1$ or $\tilde{K}_1\phi_1$.

Table 2 lists the optimal constructs for different optimization objectives (i.e. the minimizations of maximum pressure difference and mass entransy dissipation rate) with n=2, $\tilde{R}=4$, $\tilde{K}_0=\tilde{K}_1=1000$ and $\phi_1=0.1$. From the table one can see that the two optimal constructs are different. The optimal construct based on the minimization of entransy dissipation rate can decrease the mean flow resistance, with an improvement in the mass transfer performance.

4.1.3 Branch-patterned disc without the premise of optimized last-order construct

The optimal aspect ratio of the elemental sector is used to assemble the branch-patterned disc in the former subsection. In this subsection, this aspect ratio is not specified, but to be optimized. The branch-patterned disc of the first-order assembly is optimized again by relaxing the premise of optimized last-order construct and taking the aspect ratio of the elemental sector, H_0/R_0, as a new freedom. H_0/R_0 and H_1/R_1 both vary.

Based on the same elemental area and the same amounts and properties of high-permeability materials, one compares $\tilde{\tilde{f}}_{1,\min}$ with $\tilde{\tilde{f}}_0$ as shown in Figure 22. The dimensionless radius of the radial-patterned disc is (cf. eq. (50))

$$\tilde{R}=(5\tilde{K}_0\phi_1)^{1/4}/2. \tag{64}$$

When $\tilde{K}_0$ and ϕ_1 are fixed, the dimensionless radius $\tilde{R}$ can be obtained from eq. (64), and the dimensionless mean flow resistance $\tilde{\tilde{f}}_0$ of the radial-patterned disc can be obtained from Figure 22. The dimensionless mean flow resistance $\tilde{\tilde{f}}_{1,\min}$ of the branch-patterned disc decreases with the increase in $\tilde{R}$. Noted that $\tilde{\tilde{f}}_0(\tilde{R})$ is not the critical curve that distributes the high-conductivity material according to optimized radial or branch patterns, which is

Table 2 Optimal constructs for different optimization objectives

Optimization objectives	$\phi_{0,opt}$	$\tilde{D}_{opt}$	$\Delta\tilde{\tilde{P}}_{1,min}$
Minimization of maximum pressure difference	0.097	2.2292	0.0704
Minimization of entransy dissipation rate	0.084	2.8775	0.0695

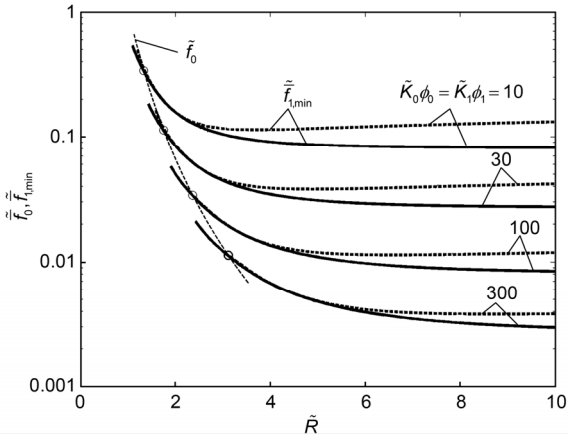

Figure 22 Effects of $\tilde{K}_0$, $\tilde{K}_1$ and ϕ_1 on dimensionless mean flow resistances of radial-patterned and branch-patterned discs.

different from the case for the premise of optimized last-order construct. For the case of the curve, $\tilde{\tilde{f}}_{1,\min}(\tilde{R})$, with $\tilde{K}_0\phi_1 = \tilde{K}_1\phi_1 = 100$, when $\tilde{R} \leqslant 2.2$ each branch-patterned disc will be reduced into a radial-patterned disc and $\tilde{R} = 2.36$ is not its critical point. Therefore, when the dimensionless radius $\tilde{R}$ exceeds that of the optimized branch-patterned disc, lower mean flow resistance is achieved when the high-permeability material is distributed according to the branch pattern. The mean flow resistance can also be decreased and the mass transfer performance of the porous media is improved by increasing $\tilde{K}_0\phi_1$ or $\tilde{K}_1\phi_1$.

4.2 Mass entransy dissipation rate minimization for "volume-to-point" mass transfer process [187]

4.2.1 Constructal mass entransy dissipation rate minimization based on constant high-permeability channels

The rectangular element, first-order assembly and second order assembly with constant channels are shown in Figures 23–25. The main optimized results are summarized in Table 3, and the optimized results based on the minimization of maximum pressure difference are summarized in Table 4 [186]. In these tables $C_i = \tilde{K}_i\phi_i$ indicates dimensionless flow conductance [186] of each high-permeability layer. Generally, $C_i/C_{i-1} >> 1$.

From these tables, one can see that the mean pressure differences are all 2/3 of the maximum pressure differences for the rectangular element, first-order assembly and second order assembly. It is interesting that the optimal constructs based on the minimization of entransy dissipation are the same as those based on minimization of maximum pressure difference [186]. When the thermal current density in the high conductive link is linear with the length, it is found that the optimal constructs based on the minimizations of entransy dissipation rate and maximum temperature difference for the heat transfer process are equal to each other [41]. Analogizing mass transfer process with heat transfer process, due to the linear distribution of the mass current density in the high-permeability layer ($n_{i,\text{opt}} >> 1$), the optimal constructs based on the two optimization objectives are identical with each other in this paper.

4.2.2 Constructal mass entransy dissipation rate minimization based on tapered high-permeability channels

The rectangular element, first-order assembly and second order assembly with tapered channels are shown in Figures 26–28. The main optimized results are summarized in Table 5,

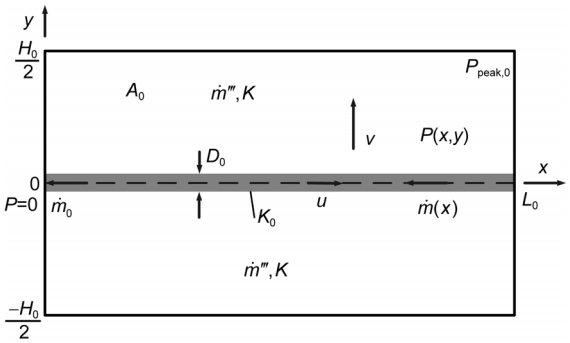

Figure 23 Rectangular element [186].

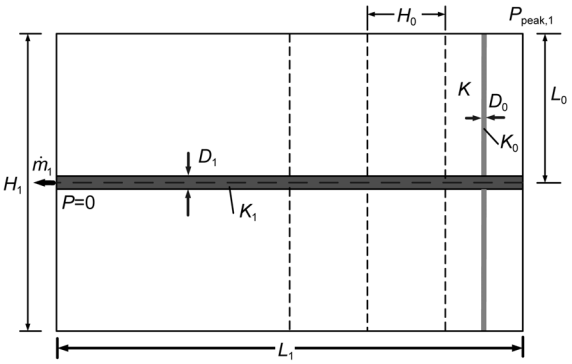

Figure 24 First-order assembly [186].

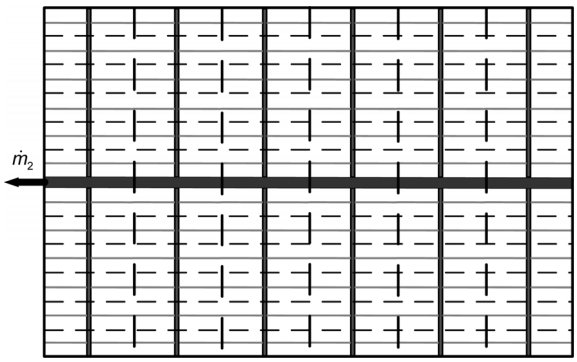

Figure 25 Second-order assembly.

Table 3 Optimal constructs based on entransy dissipation rate minimization

The order of the assembly, i	H_i/L_i	$\tilde{H}_i$	$\tilde{L}_i$	n_i	$\Delta\tilde{\tilde{P}}_i$	$\Delta\tilde{P}_i$ a)
0	$2C_0^{-1/2}$	$2^{1/2}C_0^{-1/4}$	$2^{-1/2}C_0^{1/4}$	–	$\frac{1}{3}C_0^{-1/2}$	$\frac{1}{2}C_0^{-1/2}$
1	$\left(\frac{2C_0}{C_1}\right)^{1/2}$	$2^{1/2}C_0^{1/4}$	$\frac{C_1^{1/2}}{C_0^{1/4}}$	$2^{1/2}C_1^{1/2}$	$\frac{2^{1/2}}{3}(C_0C_1)^{-1/2}$	$(2C_0C_1)^{-1/2}$
2	$\left(\frac{2C_1}{C_2}\right)^{1/2}$	$2\frac{C_1^{1/2}}{C_0^{1/4}}$	$\frac{2^{1/2}C_2^{1/2}}{C_0^{1/4}}$	$2\left(\frac{C_2}{C_0}\right)^{1/2}$	$\frac{2^{1/2}}{3}(C_1C_2)^{-1/2}$	$(2C_1C_2)^{-1/2}$
$i\geqslant 2$	$\left(\frac{2C_{i-1}}{C_i}\right)^{1/2}$	$2^{i/2}\frac{C_{i-1}^{1/2}}{C_0^{1/4}}$	$2^{\frac{i-1}{2}}\frac{C_i^{1/2}}{C_0^{1/4}}$	$2\left(\frac{C_i}{C_{i-2}}\right)^{1/2}$	$\frac{2^{1/2}}{3}(C_{i-1}C_{i-2})^{-1/2}$	$(2C_{i-1}C_{i-2})^{-1/2}$

a) These results are derived from the results of ref. [186]

Table 4 Optimal constructs based on maximum pressure difference minimization [186]

The order of the assembly, i	H_i/L_i	$\tilde{H}_i$	$\tilde{L}_i$	n_i	$\Delta\tilde{\tilde{P}}_i$	$\Delta\tilde{P}_i$
0	$2C_0^{-1/2}$	$2^{1/2}C_0^{-1/4}$	$2^{-1/2}C_0^{1/4}$	–	$\frac{1}{3}C_0^{-1/2}$	$\frac{1}{2}C_0^{-1/2}$
1	$\left(\frac{2C_0}{C_1}\right)^{1/2}$	$2^{1/2}C_0^{1/4}$	$\frac{C_1^{1/2}}{C_0^{1/4}}$	$2^{1/2}C_1^{1/2}$	$\frac{2^{1/2}}{3}(C_0C_1)^{-1/2}$	$(2C_0C_1)^{-1/2}$
2	$\left(\frac{2C_1}{C_2}\right)^{1/2}$	$2\frac{C_1^{1/2}}{C_0^{1/4}}$	$\frac{2^{1/2}C_2^{1/2}}{C_0^{1/4}}$	$2\left(\frac{C_2}{C_0}\right)^{1/2}$	$\frac{2^{1/2}}{3}(C_1C_2)^{-1/2}$	$(2C_1C_2)^{-1/2}$
$i\geqslant 2$	$\left(\frac{2C_{i-1}}{C_i}\right)^{1/2}$	$2^{i/2}\frac{C_{i-1}^{1/2}}{C_0^{1/4}}$	$2^{\frac{i-1}{2}}\frac{C_i^{1/2}}{C_0^{1/4}}$	$2\left(\frac{C_i}{C_{i-2}}\right)^{1/2}$	$\frac{2^{1/2}}{3}(C_{i-1}C_{i-2})^{-1/2}$	$(2C_{i-1}C_{i-2})^{-1/2}$

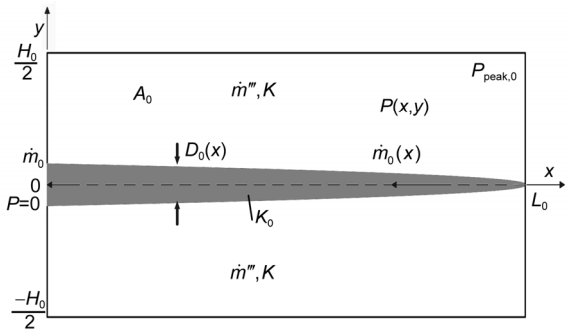

Figure 26 Rectangular element with tapered high-permeability channel.

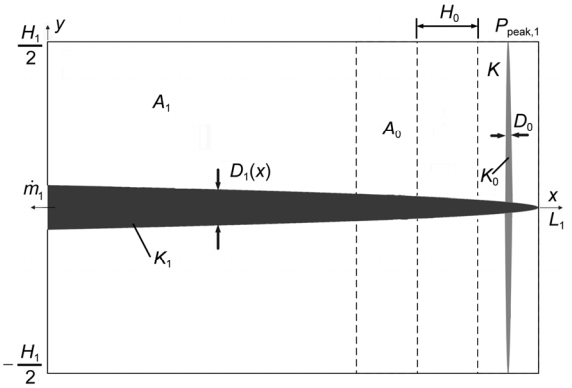

Figure 27 First-order assembly.

while the optimized results based on the minimization of maximum pressure difference are summarized in Table 6 [186], where $C_i = \tilde{K}_i\phi_i$ is the dimensionless flow conductance of the corresponding channel [186], and $\tilde{D}_i = 3\phi_i(\tilde{L}_i - \tilde{x})^{1/2}/(2\tilde{L}_i^{3/2})$. From Figures 5 and 6, one can see that the optimal constructs based on the two optimization objectives are different from each other.

(1) Compared with the rectangular element based on the minimization of maximum pressure difference, the element based on the minimization of entransy dissipation rate is more slender, and the corresponding mean pressure difference is smaller.

(2) The first-order assemblies based on the minimizations of entransy dissipation rate and maximum pressure difference, respectively, have the same optimal aspect ratio. However, the number of rectangular elements assembling the first-order assembly based on the minimization of entransy dissipation rate is more and the corresponding mean pressure difference is smaller.

(3) The *i*th-order assemblies based on the minimizations of entransy dissipation rate and maximum pressure difference, respectively, have the same optimal aspect ratio and the number of last-order assemblies assembling the *i*th-order assembly. However, the mean pressure difference based on the minimization of entransy dissipation rate is smaller.

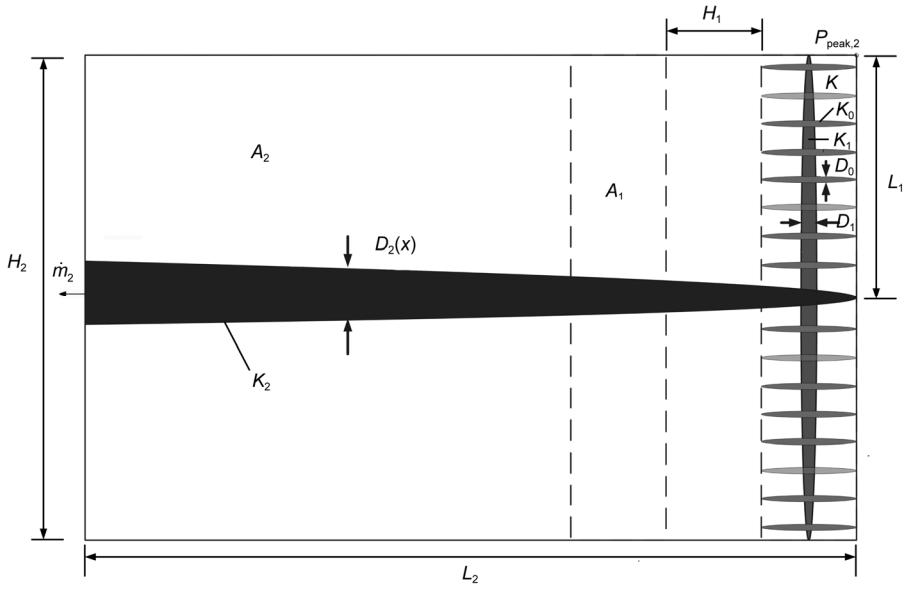

Figure 28 Second-order assembly.

Table 5 Optimal constructs based on entransy dissipation rate minimization

The order of the assembly, i	H_i/L_i	$\tilde{H}_i$	$\tilde{L}_i$	$\tilde{D}_i$	n_i	$\Delta\tilde{\tilde{P}}_i$	$\Delta\tilde{P}_i$
0	$3^{1/2}C_0^{-1/2}$	$3^{1/4}C_0^{-1/4}$	$3^{-1/4}C_0^{1/4}$	–	–	$\frac{3^{1/2}}{6}C_0^{-1/2}$	$\frac{7\sqrt{3}}{24}C_0^{-1/2}$
1	$\left(\frac{2C_0}{C_1}\right)^{1/2}$	$\frac{2}{3^{1/4}}C_0^{1/4}$	$\frac{2^{1/2}}{3^{1/4}}\frac{C_1^{1/2}}{C_0^{1/4}}$	–	$\frac{2\sqrt{6}}{3}C_1^{1/2}$	$\frac{\sqrt{2}}{4}(C_0C_1)^{-\frac{1}{2}}$	$\frac{17\sqrt{2}}{36}(C_0C_1)^{-\frac{1}{2}}$
2	$\left(\frac{2C_1}{C_2}\right)^{1/2}$	$\frac{8^{1/2}}{3^{1/4}}\frac{C_1^{1/2}}{C_0^{1/4}}$	$\frac{2}{3^{1/4}}\frac{C_2^{1/2}}{C_0^{1/4}}$	–	$2\left(\frac{C_2}{C_0}\right)^{1/2}$	$\frac{\sqrt{2}}{4}(C_1C_2)^{-\frac{1}{2}}$	$\frac{17\sqrt{2}}{36}(C_1C_2)^{-\frac{1}{2}}$
$i\geqslant 2$	$\left(\frac{2C_{i-1}}{C_i}\right)^{1/2}$	$\frac{2^{\frac{i+1}{2}}}{3^{1/4}}\frac{C_{i-1}^{1/2}}{C_0^{1/4}}$	$\frac{2^{\frac{i}{2}}}{3^{1/4}}\frac{C_i^{1/2}}{C_0^{1/4}}$	–	$2\left(\frac{C_i}{C_{i-2}}\right)^{1/2}$	$\frac{\sqrt{2}}{4}(C_{i-1}C_i)^{-\frac{1}{2}}$	$\frac{17\sqrt{2}}{36}(C_{i-1}C_i)^{-\frac{1}{2}}$

Table 6 Optimal constructs with tapered channels

The order of the assembly, i	H_i/L_i	$\tilde{H}_i$	$\tilde{L}_i$	$\tilde{D}_i$	n_i	$\Delta\tilde{\tilde{P}}_i$
0	$\frac{4\sqrt{2}}{3}C_0^{-1/2}$	$\frac{2\sqrt[4]{2}}{\sqrt{3}}C_0^{-1/4}$	$\frac{\sqrt{3}}{2\sqrt[4]{2}}C_0^{1/4}A$	–	–	$\frac{19\sqrt{2}}{90}C_0^{-1/2}$
1	$\left(\frac{2C_0}{C_1}\right)^{1/2}$	$\frac{\sqrt{3}}{\sqrt[4]{2}}C_0^{1/4}$	$\frac{\sqrt{3}\sqrt[4]{2}C_1^{1/2}}{2C_0^{1/4}}$	–	$\frac{3}{2}C_1^{1/2}$	$\frac{31\sqrt{2}(C_0C_1)^{-\frac{1}{2}}}{120}$
2	$\left(\frac{2C_1}{C_2}\right)^{1/2}$	$\sqrt{3}\sqrt[4]{2}\frac{C_1^{1/2}}{C_0^{1/4}}$	$\frac{\sqrt{3}C_2^{1/2}}{\sqrt[4]{2}C_0^{1/4}}$	–	$2\left(\frac{C_2}{C_0}\right)^{1/2}$	$\frac{31\sqrt{2}(C_1C_2)^{-\frac{1}{2}}}{120}$
$i\geqslant 2$	$\left(\frac{2C_{i-1}}{C_i}\right)^{1/2}$	$2^{\frac{2i-3}{4}}\sqrt{3}\frac{C_{i-1}^{1/2}}{C_0^{1/4}}$	$\frac{2^{\frac{2i-5}{4}}\sqrt{3}C_i^{1/2}}{C_0^{1/4}}$	–	$2\left(\frac{C_i}{C_{i-2}}\right)^{1/2}$	$\frac{31\sqrt{2}(C_{i-1}C_{i-2})^{-\frac{1}{2}}}{120}$

5 Conclusions

The mass entransy dissipation extremum principle provides a new theoretical basis for mass transfer optimization, which is different from that provided by entropy generation minimization. The mass transfer optimization results for entransy dissipation minimization in finite time thermodynamics are different from those for entropy generation minimization. In the mass transfer processes that are independent of the energy transformation, the equivalent mass

resistance and mass transfer efficiency (or mass entransy transfer efficiency) can be defined based on the mass entransy and its dissipation. Therefore, the objective of mass entransy dissipation is more suitable in the optimizations of mass transfer processes. The optimal construct based on the entransy dissipation rate minimization can decrease the mean mass transfer pressure difference to a certain extent. When the mass current density linearly distributes along the length, the relationship between the entransy dissipation rate describing global mass transfer ability of the system and the maximum pressure difference describing local mass transfer ability is linear. Additionally, both the optimal local and optimal global mass transfer performances of mass transfer structures are not always achieved simultaneously, so optimization for both of them should be paid attention in the optimization of mass transfer structure to satisfy the requirement for engineering. For the optimization of mass transfer structure, the safety restriction of mass transfer may be added. With the further development of scientific researches, the generalized entransy theory [188–190] will be more perfect and applied in a much wider field, and have more obvious advantages and greater influences on the subjects such as heat and mass transfer and other transport subjects.

It is worthwhile to note that several authors [191–198] have criticized the concept of thermal entransy in recent years. In fact, the major comments on thermal entransy were based on the misinterpretations and mistakes of some papers, and some of them lacked academic seriousness. Thermal entransy has its physical bases and advantages in heat transfer analyses and optimizations. The responses to those articles [191–198] can be seen in refs. [199–203]. Similarly, mass entransy has its physical bases and advantages in mass transfer analyses and optimizations.

The author wishes to thank the reviewers for their careful, unbiased and constructive suggestions, which led to this revised manuscript. This work was supported by the National Natural Science Foundation China (Grant Nos. 51176203 and 10905093).

1 Andresen B, Berry R S, Nitzan A, Salamon P. Thermodynamics in finite time. I. The step-Carnot cycle. Phys Rev A, 1977, 15: 2086–2093
2 Salamon P, Andresen B, Berry R S. Thermodynamics in finite time. II. Potentials for finite-time processes. Phys Rev A, 1977, 15: 2094–2101
3 Andresen B, Salamon P, Berry R S. Thermodynamics in finite time: Extremals for imperfect heat engines. J Chem Phys, 1977, 66: 1571–1578
4 Andresen B. Finite-Time Thermodynamics. Physics Laboratory II. Copenhagen: University of Copenhagen, 1983
5 Andresen B, Berry R S, Ondrechen M J, et al. Thermodynamics for processes in finite time. Acc Chem Res, 1984, 17: 266–271
6 Andresen B, Salamon P, Berry R S. Thermodynamics in finite time. Phys Today, 1984, 9: 62–70
7 Bejan A. Entropy Generation through Heat and Fluid Flow. New York: Wiley, 1982
8 Bejan A. Entropy generation minimization: The new thermodynamics of finite-size devices and finite-time processes. J Appl Phys, 1996, 79: 1191–1218
9 Bejan A, Tsatsaronis G, Moran M. Thermal Design and Optimization. New York: John Wiley Sons Inc, 1996
10 Bejan A. Entropy Generation Minimization. Boca Raton FL: CRC Press, 1996
11 Bejan A. Street network theory of organization in nature. J Adv Transport, 1996, 30: 85–107
12 Bejan A. Constructal-theory network of conducting paths for cooling a heat generating volume. Int J Heat Mass Transfer, 1997, 40: 799–816
13 Bejan A. Second law analysis in heat transfer. Energy, 1980, 5: 720–732
14 Xu Z M, Yang S R, Chen Z Q. Variational methods for optimal parameters of heat exchanger (in Chinese). Chem Eng, 1995, 46: 75–80
15 Hesselgreaves J E. Rationalisation of second law analysis of heat exchanger. Int J Heat Mass Transfer, 2000, 43: 4189–4204
16 Guo Z Y, Li Z, Zhou S Q. Uniformity principle of temperature difference field in heat exchanger (in Chinese). Sci Sin Tech, 1996, 26: 25–31
17 Guo Z Y, Zhou S Q, Li Z X, et al. Theoretical analysis and experimental confirmation of the uniformity principle of temperature difference field in heat exchanger. Int J Heat Mass Transfer, 2002, 45: 2119–2127
18 Guo Z Y, Wei S, Cheng X G. Field synergy principle for heat exchanger enhancement (in Chinese). Chin Sci Bull, 2003, 48: 2324–2327
19 Guo Z Y, Li D Y, Wang B X. A novel concept for convective heat transfer enhancement. Int J Heat Mass Transfer, 1998, 41: 2221–2225
20 Guo Z Y, Tao W Q, Shah R K. The field synergy (coordinate) principle and its applications in enhancing single phase convective heat transfer. Int J Heat Mass Transfer, 2005, 48: 1797–1807
21 Guo Z Y. Mechanism and control of convective heat transfer—Coordination of velocity and heat flow fields. Chin Sci Bull, 2001, 46: 596–599
22 Guo Z Y, Liang X G, Zhu H Y. Entransy—A physical quantity describing heat transfer ability (in Chinese). Prog Nat Sci, 2006, 16: 1288–1296
23 Guo Z Y, Zhu H Y, Liang X G. Entransy—A physical quantity describing heat transfer ability. Int J Heat Mass Transfer 2007, 50: 2545–2556
24 Guo Z Y. New physical quantities in heat (in Chinese). J Eng Thermophys, 2008, 29: 112–114
25 Guo Z Y, Cheng X G, Xia Z Z. Least dissipation of heat transport potential capacity and its application in heat conduction optimization. Chin Sci Bull, 2003, 48: 406–410
26 Han G Z, Guo Z Y. Physical mechanism of heat conduction ability dissipation and its analytical expression (in Chinese). Proc Chin Soc Electr Eng, 2007, 27: 98–102
27 Zhu H Y, Chen J Z, Guo Z Y. Electricity and thermal analogous experimental study for entransy dissipation extreme principle (in Chinese). Prog Nat Sci, 2007, 17: 1692–1698
28 Xu M T. The thermodynamic basis of entransy and entransy dissipation. Energy, 2011, 36: 4272–4277
29 Cheng X T, Liang X G, Guo Z Y. Entransy decrease principle of heat transfer in an isolated system. Chin Sci Bull, 2011, 56: 847–854
30 Cheng X T, Liang X G, Xu X H. Microcosmic expression of entransy (in Chinese). Acta Phys Sin, 2011, 60: 60512
31 Hu G J, Guo Z Y. Efficiency of heat transfer process (in Chinese). J Eng Thermophys, 2011, 32: 1005–1008
32 Hu G J, Guo Z Y. Entransy and entropy revised. Chin Sci Bull, 2011, 56: 1575–1577
33 Cheng X G, Li Z X, Guo Z Y. Variational principle in heat conduction (in Chinese). J Eng Thermophys, 2004, 25: 457–459
34 Cheng X G, Meng J A, Guo Z Y. Potential capacity dissipation minimization and entropy generation minimization in heat conduction optimization (in Chinese). J Eng Thermophys, 2005, 26: 1034–1036
35 Han G Z, Guo Z Y. Two different thermal optimization objective functions: Dissipation of heat transport potential capacity and entropy production (in Chinese). J Eng Thermophys, 2006, 27: 811–813

36 Cheng X T, Xu X H, Liang X G. Homogenization of temperature field and temperature gradient field. Sci China Ser E: Tech Sci, 2009, 52: 2937–2942
37 Ge L, Xu M T, Cheng L. Topology optimization method of volume-point problem based on entransy dissipation (in Chinese). J Eng Thermophys, 2011, 32: 993–996
38 Chen L G, Wei S H, Sun F R. Constructal entransy dissipation minimization for "volume-point" heat conduction. J Phys D: Appl Phys, 2008, 41: 195506
39 Chen L G, Wei S H, Sun F R. Constructal entransy dissipation minimization of an electromagnet. J Appl Phys, 2009, 105: 94906
40 Wei S H, Chen L G, Sun F R. The volume-point constructal optimization for discrete variable cross-section conducting path. Appl Energy, 2009, 86: 1111–1118
41 Wei S H, Chen L G, Sun F R. "Volume-point" heat conduction constructal optimization with entransy dissipation minimization objective based on rectangular element. Sci China Ser E: Tech Sci, 2008, 51: 1283–1295
42 Wei S H, Chen L G, Sun F R. Constructal multidisciplinary optimization of electromagnet based on entransy dissipation minimization. Sci China Ser E: Tech Sci, 2009, 52: 2981–2989
43 Xie Z H, Chen L G, Sun F R. Constructal optimization on T-shaped cavity based on entransy dissipation minimization. Chin Sci Bull, 2009, 54: 4418–4427
44 Xie Z H, Chen L G, Sun F R. Constructal optimization for geometry of cavity by taking entransy dissipation minimization as objective. Sci China Ser E: Tech Sci, 2009, 52: 3504–3513
45 Wei S, Chen L, Sun F. Constructal entransy dissipation minimization for "volume-point" heat conduction without the premise of optimized last-order construct. Int J Exergy 2010, 7: 627–639
46 Wei S H, Chen L G, Sun F R. Constructal entransy dissipation minimization for "volume-point" heat conduction based on triangular element. Thermal Sci, 2010, 14: 1075–1088
47 Wei S H, Chen L G, Sun F R. Constructal optimization of discrete and continuous variable cross-section conducting path based on entransy dissipation rate minimization. Sci China Tech Sci, 2010, 53: 1666–1677
48 Xiao Q H, Chen L G, Sun F R. Constructal entransy dissipation rate minimization for "disc-point" heat conduction. Chin Sci Bull, 2011, 56: 102–112
49 Chen L G, Wei S H, Sun F R. Constructal entransy dissipation rate minimization of a disc. Int J Heat Mass Transfer, 2011, 54: 210–216
50 Feng H J, Chen L G, Sun F R. "Volume-point" heat conduction constructal optimization based on entransy dissipation rate minimization with three-dimensional cylindrical element and rectangular and triangular elements at micro and nanoscales. Sci China Tech Sci, 2012, 55: 779–794
51 Feng H J, Chen L G, Sun F R. Constructal entransy dissipation rate minimization for leaf-like fins. Sci China Tech Sci, 2012, 55: 515–526
52 Xiao Q H, Chen L G, Sun F R. Constructal entransy dissipation rate minimization for heat conduction based on a tapered element. Chin Sci Bull, 2011, 56: 2400–2410
53 Xiao Q H, Chen L G, Sun F R. Constructal entransy dissipation rate minimization for umbrella-shaped assembly of cylindrical fins. Sci China Tech Sci, 2011, 54: 211–219
54 Xie Z H, Chen L G, Sun F R. Comparative study on constructal optimizations of T-shaped fin based on entransy dissipation rate minimization and maximum thermal resistance minimization. Sci China Tech Sci, 2011, 54: 1249–1258
55 Wu J, Cheng X T, Meng J A. Potential capacity dissipation extremum and minimum entropy generation in laminar flow convective heat transfer process (in Chinese). J Eng Thermophys, 2006, 27: 100–102
56 Chen Q, Ren J X. Generalized thermal resistance for convective heat transfer and its relation to entransy dissipation. Chin Sci Bull, 2008, 53: 3753–3761
57 Chen Q, Wu J, Ren J X. Thermodynamic and heat transfer optimization of convective heat transfer processes (in Chinese). J Eng Thermophys, 2008, 29: 271–274
58 Chen Q, Wang M R, Pan N, et al. Optimization principles for convective heat transfer. Energy, 2009, 34: 1199–1206
59 Wang S, Chen Q, Zhang B. A general theoretical principle for single-phase convective heat transfer enhancement. Sci China Ser E: Tech Sci, 2009, 51: 3521–3526
60 Xu M T, Guo J F, Cheng L. Application of entransy dissipation theory in heat convection. Front Energy Power Eng China, 2009, 3: 402–405
61 Wang S. Chen Q, Zhang B. An equation of entransy and its application. Chin Sci Bull, 2009, 54: 3572–3578
62 Chen H Y, Tian M S, Len X L. Numerical simulation of flow field optimization in winding pipe based on entransy dissipation extremum principle (in Chinese). In: Proceedings of Chinese Society of Engineering Thermophysics on Engineering Thermophysics and Energy Utilization, Nanjing, 2010
63 Song W M, Meng J A, Li Z X. Optimization of flue gas convective heat transfer with condensation in a rectangular channel. Chin Sci Bull, 2011, 56: 263–268
64 Chen Q, Zhu H Y, Pan N, et al. An alternative criterion in heat transfer optimization. Proc Royal Socity A: Math Phys Eng Sci, 2011, 467: 1012–1028
65 Liu W, Liu Z C, Jia H, et al. Entransy expression of the second law of thermaodynamics and its application to optimization in heat transfer process. Int J Heat Mass Transfer, 2011, 53: 3049–3059
66 Song W M, Meng J A, Li Z X. Optimization of flue gas turbulent heat transfer with condensation in a tube. Chin Sci Bull, 2011, 56: 1978–1984
67 Xiao Q H, Chen L G, Sun F R. Constructal entransy dissipation rate minimization for a heat generating volume cooled by forced convection. Chin Sci Bull, 2011, 56: 2966–2973
68 Xiao Q H, Chen L G, Sun F R. Constructal entransy dissipation rate and flow-resistance minimizations for cooling channels. Sci China Tech Sci, 2010, 53: 2458–2468
69 Li Z X, Guo Z Y. Field Synergy Principle of Heat Convection Optimization (in Chinese). Beijing: Science Press, 2010
70 Wu J, Liang X G. Application of entransy dissipation extremum principle in radiative heat transfer optimization. Sci China Ser E: Tech Sci, 2008, 51: 1306–1314
71 Cheng X T, Xu X H, Liang X G. Homogenization of temperature field for thermal radiation in space (in Chinese). J Eng Thermophys, 2010, 31: 1031–1033
72 Yu Z Q, Feng Y L, Li Z Y. Application of entransy dissipation theory in pipe solar-driven heat pump (in Chinese). In: Proceedings of Chinese Society of Engineering Thermophysics on Heat and Mass Transfer, Shanghai, 2010
73 Cheng X T, Liang X G. Entransy flux of thermal radiation and its application to enclosures with opaque surfaces. Int J Heat Mass Transfer, 2011, 54: 269–278
74 Wu J, Guo Z Y. Conversion potential energy and its application to thermodynamic optimization. Sci China Tech Sci, 2012, 55: 2169–2175
75 Wu J, Cheng X. Generalized thermal resistance and its application to thermal radiation based on entransy theory. Int J Heat Mass Transfer, 2013, 58: 374–381
76 Xia S J, Chen L G, Sun F R. Entransy dissipation minimization for liquid-solid phase processes. Sci China Tech Sci, 2010, 53: 960–968
77 Liu X B, Guo Z Y, Meng J A. Thermal resistance analysis for the heat exchangers based on entransy dissipation (in Chinese). Prog Nat Sci, 2008, 18: 1186–1190
78 Song W M, Meng J A, Liang X G, et al. Demonstration of uniformity principle of temperature difference field for one-dimensional heat exchangers (in Chinese). J Chem Ind Eng, 2008, 59: 2460–2464
79 Chen L, Chen Q, Li Z X, et al. Optimization for a heat exchanger couple based on the minimum thermal resistance principle. Int J Heat Mass Transfer, 2009, 51: 4778–4784
80 Guo J F, Cheng L, Xu M T. Entransy dissipation number and its application to heat exchanger performance evaluation. Chin Sci Bull, 2009, 54: 2708–2713
81 Liu X B, Guo Z Y. A novel method for heat exchanger analysis (in Chinese). Acta Phys Sin, 2009, 58: 4766–4771

82 Liu X B, Meng J A, Guo Z Y. Entropy generation extremum and entransy dissipation extremum for heat exchanger optimization. Chin Sci Bull, 2009, 54: 943–947
83 Xu M t, Cheng L, Guo J F. Application of entransy dissipation theory in heat exchanger design (in Chinese). J Eng Thermophys, 2009, 30: 2090–2092
84 Guo Z Y, Liu X B, Tao W Q, et al. Effectiveness–thermal resistance method for heat exchanger design and analysis. Int J Heat Mass Transfer, 2010, 53: 2877–2884
85 Guo J F, Xu M T, Cheng L. Principle of equipartition of entransy dissipation for heat exchanger design. Sci China Tech Sci, 2010, 53: 1309–1314
86 Guo J F, Xu M T, Cheng L. The entransy dissipation minimization principle under given heat duty and heat transfer area conditions. Chin Sci Bull, 2011, 56: 2071–2076
87 Li M X, Guo J F, Xu M, et al. Application of entransy dissipation theory in shell-and-tube exchanger (in Chinese). J Eng Thermophys, 2010, 31: 1189–1192
88 Qian X D, Li Z X. Analysis of entransy dissipation in heat exchangers. Int J Thermal Sci, 2011, 50: 608–614
89 Chen Q, Wu J, Wang M R, et al. A comparison of optimization theories for energy conservation in heat exchanger groups. Chin Sci Bull, 2011, 56: 449–454
90 Cheng X T, Xu X H, Liang X G. Application of entransy to optimization design of parallel thermal network of thermal control system in spacecraft. Sci China Tech Sci, 2011, 54: 964–971
91 Guo J F, Xu M T, Cheng L. Effect of temperature-dependent viscosity on the entransy of both fluids in heat exchangers. Chin Sci Bull, 2011, 56: 1934–1939
92 Guo J F, Xu M T, Cheng L. The influence of viscous heating on the entransy in two-fluid heat exchangers. Sci China Tech Sci, 2011, 54: 1267–1274
93 Guo J F, Xu M T, Cheng L. Optimization and design of plate-fin heat exchanger based on the minimum entransy dissipation number (in Chinese). J Eng Thermophys, 2011, 32: 827–831
94 Li X, Guo J F, Xu M T, et al. Entransy dissipation minimization for optimization of heat exchanger design. Chin Sci Bull, 2011, 56: 2174–2178
95 Xia S J, Chen L G, Sun F R. Optimization for entransy dissipation minimization in heat exchanger. Chin Sci Bull, 2009, 54: 3587–3595
96 Xia S J, Chen L G, Sun F R. Optimal paths for minimizing entransy dissipation during heat transfer processes with generalized radiative heat transfer law. Appl Math Model, 2010, 34: 2242–2255
97 Xia S J, Chen L G, Sun F R. Inverse optimization of heat exchange processes for minimum entransy dissipation (in Chinese). In: Proceedings of Chinese Society of Engineering Thermophysics on Engineering Thermophysics and Energy Utilization, Wuhan, 2011
98 Qian X D, Li Z, Meng J A, et al. Entransy dissipation analysis and optimization of separated heat pipe system. Sci China Tech Sci, 2012, 55: 2126–2131
99 Cheng X T, Wang W H, Liang X G. Optimization of heat transfer and heat-work conversion based on generalized heat transfer law. Sci China Tech Sci, 2012, 55: 2847–2855
100 Zhou B, Cheng X, Liang X. Power output analyses and optimizations of the Stirling cycle. Sci China Tech Sci, 2013; 56: 228–236
101 Wang W H, Cheng X T, Liang X G. Entransy dissipation, entransy-dissipation-based thermal resistance and optimization of one-stream hybrid thermal network. Sci China Tech Sci, 2013, 56: 529–536
102 Zheng Z J, He Y L, Li Y S. An entransy dissipation-based optimization principle for solar power tower plants. Sci China Tech Sci, 2014, 57: 773–783
103 Yang A B, Chen L G, Xia S J, et al. The optimal configuration of reciprocating engine based on maximum entransy loss. Chin Sci Bull, 2014, 59: 2031–2038
104 Wei S H, Chen L G, Sun F R. Constructal entransy dissipation rate minimization of round tube heat exchanger cross-section. Int J Thermal Sci, 2011, 50: 1285–1292
105 Xiao Q H, Chen L G, Sun F R. Constructal design for a steam generator based on entransy dissipation extremum principle. Sci China Tech Sci, 2011, 54: 1462–1468
106 Feng H J, Chen L G, Xie Z H, et al. Thermal insulation constructal optimization for steel rolling reheating furnace wall based on entransy dissipation extremum principle. Sci China Tech Sci, 2012, 55: 3322– 3333
107 Feng H J, Chen L G, Xie Z H, et al. Constructal optimization for H-shaped multi-scale heat exchanger based on entransy theory. Sci China Tech Sci, 2013, 56: 299–307
108 Feng H J, Chen L G, Xie Z H, et al. Generalized constructal optimization for secondary cooling process of slab continuous casting based on entransy theory. Sci China Tech Sci, 2014, 57: 784–795
109 Feng H J, Chen L G, Xie Z H, et al. Constructal entransy optimizations for insulation layer of steel rolling reheating furnace wall with convective and radiative boundary conditions. Chin Sci Bull, 2014, 59: 2470–2477
110 Chen Q, Liang X G, Guo Z Y. Entransy—A novel theory in heat transfer analysis and optimization. In: dos Santos Bernardes M A, ed. Developments in Heat Transfer. Rijeka, Croatia: InTech-Open Access Publisher, 2011. 349–372
111 Li Z X, Guo Z Y. Optimization principles for heat convection. In: Wang L Q, ed. Advances in Transport Phenomena. Berlin: Springer-Verlag, 2011. 1–91
112 Chen L G. Progress in entransy theory and its application. Chin Sci Bull, 2012, 57: 4404–4426
113 Chen Q, Liang X G, Guo Z Y. Entransy theory for the optimization of heat transfer — A review and update. Int J Heat Mass Transfer, 2013, 63: 65–81
114 Chen Q. Irreversibility and optimization of convective transport processes (in Chinese). Ph.D. Dissertation. Beijing: Tsinghua University, 2008
115 Chen Q, Ren J X, Guo Z Y. The extremum principle of mass entransy dissipation and its application to decontamination ventilation designs in space station cabins. Chin Sci Bull, 2009, 54: 2862–2870
116 Chen Q, Ren J X, The extremum principle of mass transfer potential capacity dissipation and optimization of decontamination ventilation process (in Chinese). J Eng Thermophys, 2007, 28: 505–507
117 Chen Q, Meng J A. Field synergy analysis and optimization of the convective mass transfer in photocatalytic oxidation reactors. Int J Heat Mass Transfer, 2008, 51: 2863–2870
118 Chen Q, Ren J X, Guo Z Y. Field synergy analysis and optimization of decontamination ventilation designs. Int J Heat Mass Transfer, 2008, 51: 873–881
119 Chen Q, Yang K, Wang M R, et al. A new approach to analysis and optimization of evaporative cooling system I: Theory. Energy, 2010, 35: 2448–2454
120 Chen L, Chen Q, Li Z X, et al. Moisture transfer resistance method for liquid desiccant dehumidification analysis and optimization. Chin Sci Bull, 2010, 55: 1445–1453
121 Jiang Y, Liu X H, Xie X Y. Thermological analysis frame in thermal-hygro environmental building (in Chinese). Heat Ventilat Air Condition, 2011, 41: 1–12
122 Jiang Y, Xie X Y, Liu X H. Thermological principle of moist air heat and moisture conversion processes (in Chinese). Heat Ventilat Air Condition, 2011, 41: 51–64
123 Xie X Y, Jiang Y. Thermological analysis of chilled water by evaporative cooling processes (in Chinese). Heat Ventilat Air Condition, 2011, 41: 65–76
124 Chen Q, Pan N, Guo Z Y. A new approach to analysis and optimization of evaporative cooling system II: Applications. Energy, 2011, 36: 2890–2898
125 Yuan F, Chen Q. Optimization criteria for the performance of heat and mass transfer in indirect evaporative cooling systems. Chin Sci Bull, 2012, 57: 687–693
126 Meng J A, Zeng H, Li Z X. Analysis of condenser venting rates based on the air mass entransy increases. Chin Sci Bull, 2014, 59: 3283– 3291
127 Xia S J, Chen L G, Sun F R. Entransy dissipation minimization for a class of one-way isothermal mass transfer processes. Sci China Tech Sci, 2011, 54: 352–361

128 Xia S J, Chen L G, Sun F R. Entransy dissipation minimization for one-way isothermal mass transfer processes with a generalized mass transfer law. Sci Iran Trans C Chem Chem Eng, 2012, 19: 1616–1625

129 Xia S J, Chen L G, Sun F R. Mass entransy dissipation minimization for a class of two-way isothermal equimolar mass transfer processes (in Chinese). In: Proceedings of 20th National Engineering Thermophysics Conference of Chinese Higher School, Qingdao, China, 2014. Paper No. A-14027

130 Xia S J, Chen L G, Ge Y L, et al. Entransy dissiaption minimization for isothermal throttling process (in Chinese). Acta Phys Sin, 2013, 62: 180202

131 Xia S J, Chen L G, Sun F R. Entransy dissipation minimization for isothermal crystallization processes with diffusive mass transfer law (in Chinese). J Mech Eng, 2013, 49: 175–182

132 Xia S J. Generalized thermodynamic dynamic optimization for irreversible processes and cycles. Ph.D. Dissertation. Wuhan: Naval University of Engineering, 2012

133 Andresen B. Current trends in finite-time thermodynamics. Angew Chem Int Ed, 2011, 50: 2690–2704

134 Feidt M. Thermodynamics of energy systems and processes: A review and perspectives. J Appl Fluid Mech, 2012, 5: 85–98

135 Chen L G, Wu C, Sun F R. Finite time thermodynamic optimization or entropy generation minimization of energy systems. J Non-Equil Thermodyn, 1999, 22: 327–359

136 Feidt M. Thermodynamique et Optimisation Energetique des Systems et Procedes. 2nd Ed. Paris: Technique et Documentation, Lavoisier, 1996

137 Durmayaz A, Sogut O S, Sahin B, et al. Optimization of thermal systems based on finite-time thermodynamics and thermoeconomics. Prog Energy Combust Sci, 2004, 30: 175–217

138 Bejan A. Advanced Engineering Thermodynamics. New York: Wiley, 1997

139 Berry R S, Kazakov V A, Sieniutycz S, et al. Thermodynamic Optimization of Finite Time Processes. Chichester: Wiley, 1999

140 Wu C, Chen L G, Chen J C. Recent Advances in Finite Time Thermodynamics. New York: Nova Science Publishers, 1999

141 Chen L G, Sun F R. Advances in Finite Time Thermodynamics: Analysis and Optimization. New York: Nova Science Publishers, 2004

142 Chen L G. Finite-Time Thermodynamic Analysis of Irreversible Processes and Cycles (in Chinese). Beijing: Higher Education Press, 2005

143 Wu F, Chen L G, Sun F. Finite Time Thermodynamic Optimization for Stirling Machines (in Chinese). Beijing: Chemical Industry Press, 2008

144 Wang J, He J Z, Mao Z. Performance of a quantum heat engine cycle working with harmonic oscillator systems. Sci China Ser G: Phys Mech Astron, 2007, 50: 163–176

145 Song H J, Chen L G, Sun F R. Optimal configuration of a class of endoreversible heat engines for maximum efficiency with radiative heat transfer law. Sci China Ser G: Phys Mech Astron, 2008, 51: 1272–1286

146 Xia D, Chen L G, Sun F R. Optimal performance of a generalized irreversible four-reservoir isothermal chemical potential transformer. Sci China Ser B: Chemistry, 2008, 51: 958–970

147 Li J, Chen L G, Sun F R. Optimal configuration for a finite high-temperature source heat engine cycle with complex heat transfer law. Sci China Ser G: Phys Mech Astron, 2009, 52: 587–592

148 Xia S J, Chen L G, Sun F R. Optimal path of piston motion for Otto cycle with linear phenomenological heat transfer law. Sci China Ser G: Phys Mech Astron, 2009, 52: 708–719

149 Xia S J, Chen L G, Sun F R. Maximum power output of a class of irreversible non-regeneration heat engines with a non-uniform working fluid and linear phenomenological heat transfer law. Sci China Ser G: Phys Mech Astron, 2009, 52: 1961–1970

150 He J Z, He X, Tang W. The performance characteristics of an irreversible quantum Otto harmonic cycles. Sci China Ser G: Phys Mech Astron, 2009, 52: 1317–1323

151 Liu X W, Chen L G, Wu F, et al. Ecological optimization of an irreversible harmonic oscillators Carnot heat engine. Sci China Ser G: Phys Mech Astron, 2009, 52: 1976–1988

152 Ding Z M, Chen L G, Sun F R. Thermodynamic characteristic of a Brownian heat pump in a spatially periodic temperature field. Sci China Phys Mech Astron, 2010, 53: 876–885

153 Ge Y L, Chen L G, Sun F R. Optimal paths of piston motion of irreversible Otto cycle heat engines for minimum entropy generation (in Chinese). Sci China Phys Mech Astron, 2010, 40: 1115–1129

154 Ding Z M, Chen L G, Sun F R. Modeling and performance analysis of energy selective electron (ESE) engine with heat leakage and transmission probability. Sci China Phys Mech Astron, 2011, 54: 1925–1936

155 Shu L W, Chen L G, Sun F R. The minimal average heat consumption for heat-driven binary separation process with linear phenomenological heat transfer law. Sci China Ser B: Chem, 2009, 52: 1154–1163

156 Ma K, Chen L G, Sun F R. Optimal paths for a light-driven engine with linear phenomenological heat transfer law. Sci China Chem, 2010, 53: 917–926

157 Xia S J, Chen L G, Sun F R. Hamilton-Jacobi-Bellman equations and dynamic programming for power-optimization of multistage heat engine system with generalized convective heat transfer law. Chin Sci Bull, 2011, 56: 1147–1157

158 Tsirlin A M. Optimum control of irreversible thermal and mass-transfer processes. Sov J Comput Syst Sci, 1992, 30: 23–31

159 Tsirlin A M, Kazakov V A, Berry R S. Finite-time thermodynamics: Limiting performance of rectification and minimal entropy production in mass transfer. J Phys Chem, 1994, 98: 3330–3336

160 Tsirlin A M, Mironova V A, Amelkin S A, et al. Finite-time thermodynamics: Conditions of minimal dissipation for thermodynamic process with given rate. Phys Rev E, 1998, 58: 215–223

161 Tsirlin A M, Kazakov V A, Zubov D V. Finite-time thermodynamics: Limiting possibilities of irreversible separation processes. J Phys Chem, 2002, 106: 10926–10936

162 Tsirlin A M, Kazakov V A. Irreversible work of separation and heat-driven separation. J Phys Chem, 2004, 108: 6035–6042

163 Tsirlin A M, Kazakov V A, Romanova T S. Optimal separation sequence for three-component mixtures. J Phys Chem, 2007, 111: 3178–3182

164 Tsirlin A M, Grigorevsky I N. Thermodynamical estimation of the limiting potential of irreversible binary distillation. J Non-Equil Thermodyn, 2010, 35: 213–234

165 Tsirlin A M, Leskov E E, Kazakov V A. Finite-time thermodynamics: Limiting performance of diffusion engines and membrane systems. J Phys Chem A, 2005, 109: 9997–10003

166 Xia S J, Chen L G, Sun F R. Maximum power configuration for multi-reservoir chemical engines. J Appl Phys, 2009, 105: 124905

167 167 Xia S J, Chen L G, Sun F R. Optimal configuration of a finite mass reservoir isothermal chemical engine for maximum work output with linear mass transfer law. Rev Mexic de Fisica, 2009, 55: 399–408

168 Xia S J, Chen L G, Sun F R. Maximum work configurations of finite potential reservoir chemical engines. Sci China Chem, 2010, 53: 1168–1176

169 Xia D, Chen L G, Sun F R. Unified description of isothermal endoreversible chemical cycles with linear mass transfer law. Int J Chem React Eng, 2012, 9: A106

170 Shen W D, Jiang Z M, Tong J G. Engineering Thermodynamics (in Chinese). Beijing: Higher Education Press, 2000

171 Bejan A. How nature takes shape: extensions of constuctal theory to ducts, river, turbulence, cracks, dendritic crystals and spatial economics. Int J Thermal Sci, 1999, 38: 653–663

172 Bejan A. From heat transfer principles to shape and structure in nature: Constructal theory. J Heat Transfer, 2000, 122: 430–449

173 Bejan A, Lorente S. Thermodynamic optimization of flow geometry in mechanical and civil engineering. J Non-Equil Thermodyn, 2001, 26: 305–354

174 Bejan A, Lorente S. Constructal design and thermodynamic optimi-

zation. Ann Rev Heat Transfer, 2005, 14: 511–527
175 Bejan A, Lorente S. Constructal theory of generation of configuration in nature and engineering. J Appl Phys, 2006, 100: 41301
176 Reis A H. Constructal theory: From engineering to physics, and how flow systems develop shape and structure. Appl Mech Rev, 2006, 59: 269–282
177 Bejan A, Merkx G W. Constructal Theory of Social Dynamics. New York: Springer, 2007
178 Bejan A, Lorente S. Design with Constructal Theory. New Jersey: Wiley, 2008
179 Lorenzini G, Moretti S, Conti A. Fin Shape Thermal Optimization Using Bejan's Constructal Theory. San Trancisco, USA: Morgan & Claypool Publishers, 2011
180 Chen L G. Progress in study on constructal theory and its application. Sci China Tech Sci, 2012, 55: 802–820
181 Bejan A, Zane P J. Design in Nature. New York: Doubleday, 2012
182 Rocha L A O, Lorente S, Bejan A. Constructal Law and the Unifying Principle of Design. Berlin: Springer, 2013
183 Bejan A, Lorente S. Constructal law of design and evolution: Physics, biology, technology, and society. J Appl Phys, 2013, 113: 151301
184 Miguel A F. The emergence of design in pedestrian dynamics: Locomotion, self-organization, walking paths and constructal law. Phys Life Rev, 2013, 10: 168–190
185 Luo L A. Heat and Mass Transfer Intensification and Shape Optimization. New York: Springer, 2013
186 Bejan A, Errera M R. Deterministic tree networks for fluid flow: Geometry for minimal flow resistance between a volume and one point. Fractals, 1997, 55: 685–695
187 Xiao Q H. Constructal optimizations for heat and mass transfer based on entransy dissipation extremum principle. Ph.D. Dissertation. Wuhan: Naval University of Engineering, 2011
188 Liu X B, Wang M, Meng J, et al. Minimum entransy dissipation principle for the optimization of transport networks. Int J Nonlin Sci Numer Simul, 2010, 11: 113–120
189 Cheng X T, Xu X, Liang X G. Principles of potential entransy in generalized flow (in Chinese). Acta Phys Sin, 2011, 60: 118103
190 Cheng X T, Dong Y, Liang X G. Potential entransy and potential entransy decrease principle (in Chinese). Acta Phys Sin, 2011, 60: 114402
191 Grazzini G, Borchiellini R, Lucia U. Entropy versus entransy. J Non-Equil Thermodyn, 2013, 38: 259–271
192 Lucia U. Stationary open systems: A brief review on contemporary theories on irreversibility. Physica A, 2013, 392: 1051–1062
193 Herwig H. Do we really need "entransy"? A critical assessment of a new quantity in heat transfer analysis. J Heat Transfer, 2014, 136: 045501
194 Bejan A."Entransy," and its lack of content in physics. J Heat Transfer, 2014, 136: 055501
195 Awad M M. Discussion: "Entransy is Now Clear". J Heat Transfer, 2014, 136: 095502
196 Grazzini G, Rocchetti A. Thermodynamic optimization of irreversible refrigerators. Energy Convers Manag, 2014, 84: 583–588
197 Manjunath K, Kaushik S C. Second law thermodynamic study of heat exchangers: A review. Renew Sustain Energy Rev, 2014, 40: 348–374
198 Awad M M. Entransy unmasked. Energy Convers Manag, 2014, 88: 1070–1071
199 Guo Z Y, Chen Q, Liang X G. Closure to "Discussion of 'Do we really need "entransy"?'". J Heat Transfer, 2014, 136: 046001
200 Guo Z Y. Closure to "Discussion of 'Entransy', and its lack of content in physics" (2014, ASME J. Heat Transfer, 136(5), p. 055501). J Heat Transfer, 2014, 136: 056001
201 Chen Q, Guo Z Y, Liang X G. Closure to "Discussion of 'Entransy is Now Clear'" (2014, ASME J. Heat Transfer, 136(9), p. 095502). J Heat Transfer, 2014, 136: 096001
202 Cheng X T, Liang X G. Reply to "Entransy unmasked" by Awad. Energy Convers Manage, 2014, 88: 1072–1073
203 Cheng X T, Chen Q, Liang X G. Comments on "Second law thermodynamic study of heat exchangers: A review" (Renew Sustain Energy Rev, 2014, 40: 348–374). Renew Sustain Energy Rev, in press